

Probing the Randall-Sundrum geometric origin of flavor with lepton flavor violation

Kaustubh Agashe^a, Andrew E. Blechman^b, Frank Petriello^c

^a*Department of Physics,
Syracuse University, Syracuse, NY 13244*

and

*School of Natural Sciences,
Institute for Advanced Study,
Princeton, NJ 08540*

^b*Department of Physics,
The Johns Hopkins University,
Baltimore, MD 21218*

^c*Department of Physics,
University of Wisconsin,
Madison, WI 53706*

Abstract

The “anarchic” Randall-Sundrum model of flavor is a low energy solution to both the electroweak hierarchy and flavor problems. Such models have a warped, compact extra dimension with the standard model fermions and gauge bosons living in the bulk, and the Higgs living on or near the TeV brane. In this paper we consider bounds on these models set by lepton flavor violation constraints. We find that loop-induced decays of the form $l \rightarrow l' \gamma$ are ultraviolet sensitive and uncalculable when the Higgs field is localized on a four-dimensional brane; this drawback does not occur when the Higgs field propagates in the full five-dimensional space-time. We find constraints at the few TeV level throughout the natural range of parameters, arising from $\mu - e$ conversion in the presence of nuclei, rare μ decays, and rare τ decays. A “tension” exists between loop-induced dipole decays such as $\mu \rightarrow e \gamma$ and tree-level processes such as $\mu - e$ conversion; they have opposite dependences on the five-dimensional Yukawa couplings, making it difficult to decouple flavor-violating effects. We emphasize the importance of the future experiments MEG and PRIME. These experiments will definitively test the Randall-Sundrum geometric origin of hierarchies in the lepton sector at the TeV-scale.

I. INTRODUCTION

The Standard Model (SM) of particle physics is a remarkably successful description of nature. However, it contains several unsatisfactory features. In particular, there are many hierarchies built into the model that have no *a priori* explanation. The most famous of these is the huge separation between the electroweak and Planck scales. There have been many proposed solutions to this problem. One possibility is the Randall-Sundrum scenario (RS) [1]. In this model, our four-dimensional space-time is embedded into a five-dimensional anti de-Sitter space. The extra “warped” fifth dimension is compactified on an orbifold. This space-time is described by the metric

$$ds^2 = e^{-2kr_c\phi} \eta_{\mu\nu} dx^\mu dx^\nu - r_c^2 d\phi^2, \quad (1)$$

where $-\pi \leq \phi \leq \pi$. Three-branes are placed at the orbifold fixed points $\phi = 0$ and $\phi = \pi$ (and its reflection at $\phi = -\pi$). The brane at $\phi = 0$ is called the Planck or ultraviolet (UV) brane, while the brane at $\phi = \pi$ is called the TeV or infrared (IR) brane. For sizes of the fifth dimension $kr_c \sim 11 - 12$, the TeV scale is obtained from the fundamental Planck scale via an exponential warping induced by the anti de-Sitter geometry: $M_{\text{TeV}} = M_{\text{pl}} e^{-k\pi r_c}$. It was shown that this setup can be naturally stabilized [2]. The original model placed all SM fields on the IR brane.

This scenario does not explain all unnatural parameters in the SM. The fermion Yukawa couplings, except for the top quark coupling, are small and hierarchical. The minimal RS model offers no solution to this flavor hierarchy problem. In addition, the flavor sector in the RS model is sensitive to ultraviolet physics, and requires a cut-off of roughly 10^3 TeV to avoid dangerous flavor-changing neutral currents. This is problematic, as the only cut-off available is the electroweak scale.

One solution to this problem is to permit some or all of the SM fields to propagate in the full $5D$ space [3, 4, 5]. The only requirement for solving the gauge hierarchy problem is to have the Higgs field localized near the IR brane. This immediately presents a solution to the flavor hierarchy problem [4, 5], since the Yukawa couplings of the Higgs field to the fermions become dependent on the position of the fermion fields relative to the IR brane. By placing fermions at different positions in the $5D$ bulk, a hierarchy in the effective $4D$ Yukawa couplings can be generated even with anarchic $\mathcal{O}(1)$ $5D$ couplings. These “anarchic” RS models set all diagonal and off-diagonal Yukawa couplings to $\mathcal{O}(1)$. In addition, allowing fermions to propagate in the bulk suppresses the operators leading to dangerous flavor changing neutral currents [5, 6]. Some collider [7] and flavor physics [8, 9, 10, 11, 12] phenomenology of these models has been considered previously.

Additional work is needed to make this scenario fully realistic. It was shown that the simplest formulation leads to large violations of the custodial symmetry in the SM [13]. There are two known solutions to this problem. The first extends the bulk gauge symmetry to $SU(2)_L \times SU(2)_R$; when broken by boundary conditions, a bulk custodial $SU(2)$ symmetry is preserved [14]. The second model introduces large brane kinetic terms to suppress precision electroweak constraints [15]. Both solutions allow for the masses of the first Kaluza-Klein (KK) excitations to be as low as 3 TeV, generating interesting phenomenology which may be observable at the upcoming Large Hadron Collider (LHC).

In this paper we probe the anarchic RS scenario by examining its effects on lepton flavor-violating observables. We study here a minimalistic model; we assume the SM gauge group, KK masses of a few TeV or larger, and an anarchic $5D$ Yukawa structure. We allow the

Higgs boson to propagate in the full $5D$ space, which encompasses features found in several recent models [16, 17]. Specific theories such as those mentioned above with a left-right symmetric bulk or large brane kinetic terms will predict slightly different effects than we find here, but we believe that our analysis captures the most important effects. We note that the flavor violation we study here is completely independent of neutrino physics parameters. We subject the anarchic RS picture to a complete set of experimental constraints: the rare μ decays $\mu \rightarrow e\gamma$ and $\mu^\pm \rightarrow e^\pm e^\mp e^\pm$, the rare τ decays $\tau \rightarrow \{e, \mu\}\gamma$ and tri-lepton decay modes, and $\mu - e$ conversion in the presence of nuclei. We find constraints on the KK scale of a few TeV throughout parameter space. Interestingly, there is a “tension” between dipole operator decays such as $l \rightarrow l'\gamma$ and the remaining processes. They have different dependences on the $5D$ Yukawa parameters, leading to strong constraints throughout parameter space. We also find that when the Higgs field is localized on the TeV brane, the dipole decays $l \rightarrow l'\gamma$ are UV sensitive and uncalculable in the RS theory. This does not occur when the Higgs boson can propagate in the full $5D$ space-time. We emphasize the important role played by several future experiments: MEG [18], which will improve the constraints on $\mu \rightarrow e\gamma$ by two orders of magnitude; PRIME [19], which will strengthen the bounds on $\mu - e$ conversion by several orders of magnitude; super- B factories, which will improve the bounds on rare τ decays by an order of magnitude. Measurements from these three experiments will definitively test the anarchic RS picture.

We briefly compare our work to previous papers on lepton flavor violation in the RS framework. Reference [20] studied lepton flavor violation in a scenario where only a right-handed neutrino propagates in the full $5D$ spacetime. The studies in [8, 12] allowed all SM fermions and gauge bosons to propagate in the bulk. Reference [8] did not incorporate custodial isospin, and therefore considered KK masses of 10 TeV, while the paper [12] considered a model with structure in the $5D$ masses and Yukawa couplings. None of these studies considered a bulk Higgs field. They also did not address the UV sensitivity of dipole decays in the brane Higgs field scenario, nor did they discuss the tension between tree-level and loop-induced processes. We also present a more detailed study of future experimental prospects than previous analyses.

This paper is organized as follows. In Section 2 we present our notation and describe the model. We discuss in Section 3 the $\mu - e$ conversion and tri-lepton decay processes, which are mediated by tree-level gauge boson mixing. We discuss the loop-induced decays $l \rightarrow l'\gamma$ in Section 4. In Section 5 we present our Monte Carlo scan over the anarchic RS parameter space. We summarize and conclude in Section 6.

II. NOTATION AND CONVENTIONS

In this section we present our notation and describe the model we consider. The basic action is

$$S = \int d^4x d\phi \sqrt{G} [\mathcal{L}_{\text{gauge}} + \mathcal{L}_{\text{fermion}} + \mathcal{L}_{\text{Higgs}}]. \quad (2)$$

The Lagrangian for gauge fields in the bulk, $\mathcal{L}_{\text{gauge}}$, has been studied in [3]. $\mathcal{L}_{\text{fermion}}$ was presented in [4, 5, 7] using an IR brane Higgs boson; we will review the relevant formulae and discuss the transition to a bulk Higgs below. Our setup of the bulk Higgs field will follow the discussion in [17].

A. Brane Higgs field

We begin by considering the case of the Higgs field localized on the IR brane. The Lagrangian in this case is

$$\mathcal{L}_{\text{Higgs}} = [D_\mu H (D^\mu H)^\dagger - V(H) - \mathcal{L}_{\text{Yukawa}}] [\delta(\phi - \pi) + \delta(\phi + \pi)], \quad (3)$$

where D_μ is the covariant derivative. $\mathcal{L}_{\text{Yukawa}}$ describes the Yukawa interactions with the fermions. The Lagrangian for bulk fermions was derived in [4, 5, 7]; it takes the form

$$\mathcal{L}_{\text{fermion}} = i\bar{\Psi} E_A^M \Gamma^A D_M \Psi - \text{sgn}(\phi) k c_\Psi \bar{\Psi} \Psi. \quad (4)$$

where E_A^M is the inverse vielbein. This Lagrangian admits zero-mode solutions. The c_Ψ parameters indicate where in the fifth dimension the zero-mode fermions are localized: either near the TeV brane ($c < 1/2$) or near the Planck brane ($c > 1/2$). The 4D Yukawa couplings of these fermions are exponentially sensitive to the c_Ψ parameters. We perform the KK decomposition of the fermion field by splitting it into chiral components, $\Psi = \Psi_L + \Psi_R$, yielding

$$\Psi_{L,R}(x, \phi) = \sum_n \frac{e^{2kr_c|\phi|}}{\sqrt{r_c}} \psi_{L,R}^{(n)}(x) f_{L,R}^{(n)}(\phi; c). \quad (5)$$

The c dependence becomes part of the KK wavefunction $f_{L,R}^{(n)}(\phi; c)$; explicit formulas for these wavefunctions can be found in [4, 5, 7].

The SM contains two types of fermions, corresponding to singlets (S) and doublets (D) under $SU(2)_L$. In the SM, we require that the S fermions are right-handed while the D fermions are left-handed. However, in five dimensions we must have both chiralities. To get a chiral zero-mode sector we use the orbifold parity of RS models. In particular, we choose (S_R, D_L) to be even under the orbifold parity (Neuman boundary conditions) and (S_L, D_R) to be odd (Dirichlet boundary conditions). The odd fields will not have zero modes, and the even zero modes will correspond to the SM fermions. We now group these fermions and their first KK modes into the vectors

$$\begin{aligned} \Psi_L^I &= (D_L^{i(0)}, D_L^{i(1)}, S_L^{i(1)}), \\ \Psi_R^I &= (S_R^{i(0)}, S_R^{i(1)}, D_R^{i(1)}), \end{aligned} \quad (6)$$

where i is a flavor index ($i = e, \mu, \tau$) and $I = 1 \dots 9$. We will show in a later section that higher KK modes have a negligible effect on our results.

The fundamental 5D Yukawa interaction is

$$\mathcal{L}_{\text{Yukawa}} = \frac{\lambda_{5D}^{ij}}{k} \bar{D}_L^i H S_R^j. \quad (7)$$

Using the vectors in Eq. 6 and substituting in the KK expansion of Eq. 5 yields

$$\mathcal{L}_{\text{Yukawa}} = \frac{\Lambda_{IJ}}{k} \bar{\Psi}_L^I H \Psi_R^J + \text{h.c.}, \quad (8)$$

where

$$\Lambda = \begin{pmatrix} \lambda_{4D} & \lambda_{4D} F_R & 0 \\ F_L \lambda_{4D} & F_L \lambda_{4D} F_R & 0 \\ 0 & 0 & 0 \end{pmatrix}. \quad (9)$$

Each internal block is a 3×3 matrix, with

$$F_{L,R} \equiv \begin{pmatrix} f_{e_{L,R}}^{(1)}/f_{e_{L,R}}^{(0)} & 0 & 0 \\ 0 & f_{\mu_{L,R}}^{(1)}/f_{\mu_{L,R}}^{(0)} & 0 \\ 0 & 0 & f_{\tau_{L,R}}^{(1)}/f_{\tau_{L,R}}^{(0)} \end{pmatrix} \quad (10)$$

These should be evaluated on the TeV brane, since that is where the Higgs is localized. We find

$$\lambda_{4D}^{ij} = \frac{\epsilon}{kr_c} f_i^{(0)} f_j^{(0)} \lambda_{5D}^{ij} = \sqrt{\frac{(1-2c_i)(1-2c_j)}{(\epsilon^{1-2c_i}-1)(\epsilon^{1-2c_j}-1)}} \epsilon^{1-(c_i+c_j)} \times \lambda_{5D}^{ij}, \quad (11)$$

where $\epsilon = e^{\pi k r_c}$ and there is no sum over i, j . It is straightforward to write down the mass matrix for the fermions:

$$\mathcal{M} = \begin{pmatrix} M_0 & M_0 F_R & 0 \\ F_L M_0 & F_L M_0 F_R & M_{KK} \\ 0 & M_{KK} & 0 \end{pmatrix}, \quad (12)$$

where $M_0^{ij} = \frac{v}{\sqrt{2}} \lambda_{4D}^{ij}$ is the zero mode mass matrix. M_{KK} is a diagonal matrix that contains the KK masses. M_0 is not diagonal. We can diagonalize this zero mode mass matrix in the usual way, by constructing a biunitary transformation (U_L, U_R) so that $M_D = U_L M_0 U_R^\dagger$ is diagonal. We can embed this rotation into the full matrix above by multiplying on the left by $\text{diag}(U_L, 1, 1)$ and on the right by $\text{diag}(U_R^\dagger, 1, 1)$. This gives

$$\mathcal{M} = \begin{pmatrix} M_D & \frac{v}{\sqrt{2}} \Delta_R & 0 \\ \frac{v}{\sqrt{2}} \Delta_L & \Delta_1 & M_{KK} \\ 0 & M_{KK} & 0 \end{pmatrix}. \quad (13)$$

We have set $\frac{v}{\sqrt{2}} \Delta_R = U_L M_0 F_R = M_D U_R F_R$ and $\frac{v}{\sqrt{2}} \Delta_L = F_L M_0 U_R^\dagger = F_L U_L^\dagger M_D$. A factor of $\frac{v}{\sqrt{2}}$ was extracted to make it easier to match to the Yukawa matrix. Notice that the middle entry can also be written in terms of the diagonal zero-mode matrix: $\Delta_1 = F_L M_0 F_R = F_L U_L^\dagger M_D U_R F_R$. From now on, we will use this expression. To find the Yukawa matrix Λ in this basis, we just divide Eq. 13 by $\frac{v}{\sqrt{2}}$ and set $M_{KK} = 0$. We note that this implies we are considering the exchange of a complex Higgs boson, which is equivalent to the exchange of the physical Higgs boson and the longitudinal component of the Z . The diagonalization of this mass matrix is discussed in the Appendix.

B. Bulk Higgs field

We now discuss the changes that occur when we allow the Higgs to propagate in the full $5D$ space. A new coupling of the Higgs boson to the fermion KK states exists: $H \bar{S}_L^{(1)} D_R^{(1)} + \text{h.c.}$ This is not present in the brane Higgs case because the S_L and D_R wavefunctions vanish identically on the TeV brane due to the Dirichlet boundary conditions. The fermion mass matrix becomes

$$\mathcal{M} = \begin{pmatrix} M_D & \frac{v}{\sqrt{2}} \Delta_R & 0 \\ \frac{v}{\sqrt{2}} \Delta_L & \Delta_1 & M_{KK} \\ 0 & M_{KK} & \Delta_2 \end{pmatrix}. \quad (14)$$

$\Delta_{L,R,1}$ are not the same as in the brane case; they now include overlap integrals of the KK and zero-mode fermion wavefunctions with the Higgs wavefunction. Δ_2 represents the wavefunction overlaps between the first KK modes of the right-handed doublet and left-handed singlet leptons; the explicit expressions as well as the details of diagonalizing \mathcal{M} can be found in the Appendix. We note that all of the Δ are proportional to the $4D$ Yukawa couplings.

Our discussion of the bulk Higgs field will follow the presentation in [17]. The $5D$ profile for the Higgs vev is

$$\chi_H(\phi) = N_H e^{2\sigma} J_\nu \left(i x_T e^{kr_c(\phi-\pi)} \right). \quad (15)$$

Here, x_T is the solution of a root equation giving the tachyonic mass, N_H is a normalization factor, $\sigma = kr_c\phi$, and ν is the index of the solution. We will simplify this further for our discussion by using the asymptotic expansion of the Bessel function for large index, $J_\nu(z) \sim z^\nu$. Using this expansion gives the following normalized profile:

$$\chi_H(\phi) = \sqrt{\frac{kr_c(1+\nu)}{e^{2(1+\nu)kr_c\pi} - 1}} e^{(2+\nu)\sigma}. \quad (16)$$

This satisfies the constraint

$$1 = 2 \int_0^\pi d\phi e^{-2\sigma} \chi_H^2(\phi), \quad (17)$$

where the factor of 2 comes from the $[-\pi, 0]$ integration. In our analysis we will vary the index ν , without worrying about its dependence on the model parameters in [17]. This also makes a connection with the A_5 composite Higgs models in [16], which is approximately realized in this framework as $\nu = 0$. We can also make a direct comparison to the TeV brane Higgs scenario, which is realized by $\nu \rightarrow \infty$.

We will now study the effect of the bulk Higgs field on the gauge boson sector. We begin with the action

$$S_{gauge} = \int d^5x \sqrt{-G} G^{MN} (D_M H)^\dagger D_N H. \quad (18)$$

Performing a standard KK decomposition, and expanding $H = v\chi_H/\sqrt{2r_c}$, we arrive at the mass matrix

$$\frac{m_0^2}{2} \sum_{m,n=0} a_{mn} A_\mu^{(m)} A^{\mu(n)}, \quad (19)$$

with

$$a_{mn} = 4\pi \int_0^\pi d\phi e^{-2\sigma} \chi_H^2 \chi^{(m)} \chi^{(n)}. \quad (20)$$

The $\chi^{(n)}$ are the usual gauge wave-functions, which can be found in [3]. We note that $\chi^{(0)} = 1/\sqrt{2\pi}$. We show in Fig. 1 the elements $f_i = a_{0i}$ of this mixing matrix. The expectation is that as $\nu \rightarrow \infty$, these should approach the brane Higgs values of $(-1)^{i+1} \sqrt{2\pi kr_c} \approx \pm 8.42$, assuming the value $kr_c = 11.27$; this is indeed what occurs.

We must now study the fermion sector, particularly what form the $4D$ Yukawa couplings take in terms of the $5D$ values. We begin with the action

$$S_{ffH} = \frac{\lambda_{5D} \sqrt{1+\nu}}{\sqrt{k}} \int d^5x \sqrt{-G} H^\dagger \psi_D \psi_S^c. \quad (21)$$

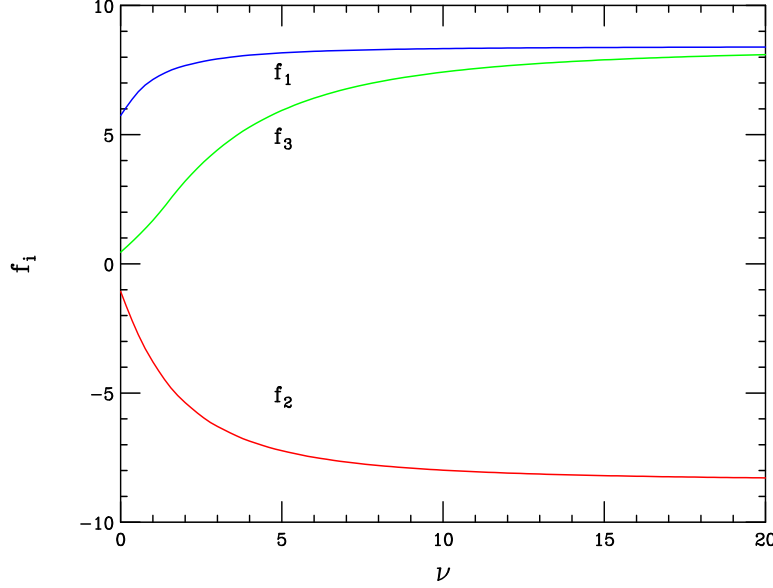


FIG. 1: f_i , the off-diagonal elements of the gauge boson mass matrix that describe the mixing of the zero-mode with the i -th KK-mode.

where the ν -dependent prefactor is included to reproduce the correct 4D Yukawa coupling as $\nu \rightarrow \infty$. The zero-mode fermion wave-function is $e^{2\sigma} f^{(0)} / \sqrt{r_c}$, where

$$f^{(0)} = \sqrt{\frac{kr_c(1-2c)}{2(e^{(1-2c)kr_c\pi} - 1)}} e^{-c\sigma}. \quad (22)$$

Inserting this into the action, and expanding H as before, we find the following expression for the 4D Yukawa:

$$\begin{aligned} \lambda_{4D} &= \frac{\lambda_{5D}(1-2c)}{e^{(1-2c)kr_c\pi} - 1} \left[\sqrt{kr_c(1+\nu)} \int_0^\pi d\phi \chi_H e^{-2c\sigma} \right] \\ &= \frac{\lambda_{5D}(1-2c)}{e^{(1-2c)kr_c\pi} - 1} \left[\frac{1+\nu}{\sqrt{e^{2(1+\nu)kr_c\pi} - 1}} \frac{e^{(2+\nu-2c)kr_c\pi} - 1}{2+\nu-2c} \right]. \end{aligned} \quad (23)$$

For simplicity, we have only presented the diagonal Yukawa coupling. To reproduce the brane Higgs diagonal Yukawa coupling in Eq. 11, the bracketed integral should reduce to $e^{(1-2c)kr_c\pi}$ as $\nu \rightarrow \infty$. It is simple to check that this occurs.

C. The anarchic RS parameters

We discuss here the parameters of the anarchic RS model and give their natural values. We first note that Eq. 11 relates the diagonal 5D Yukawa couplings to the fermion c parameters through the measured fermion masses. The off-diagonal entries are removed after diagonalization with $U_{L,R}$. The preferred size of the Yukawa couplings can be determined by demanding consistency with $Z \rightarrow b\bar{b}$ measurements and by the size of the top quark mass; this yields $\lambda_{5D} \approx 2$ [14]. We assume three couplings (Y_e, Y_μ, Y_τ) of this approximate magnitude. The size of these couplings implies $c > 1/2$ for all three leptons, indicating that

they are localized near the Planck brane. For simplicity, we take $c_L = c_R$. We note that this range of c is the appropriate one for first and second generation quarks also; for the third generation, $c_{b_L} = c_{t_L} \sim 0.45$, while $c_{b_R} \sim 0.5$ and $c_{t_R} \sim 0$ [14].

We can also estimate the natural sizes of the $U_{L,R}$ matrix elements. For illustration, we consider here a two-family scenario; it is straightforward to extend this example to three families. Assuming an anarchic RS scenario, so that all of the $\lambda_{5D}^{ij} \sim \mathcal{O}(1)$, we can use Eq. 11 to write the $4D$ Yukawa matrix as

$$\lambda_{5D} = \begin{pmatrix} Y_{11} & Y_{12} \\ Y_{12} & Y_{22} \end{pmatrix} \Rightarrow \lambda_{4D} \sim \begin{pmatrix} Y_{11} f_e^{(0)2} & Y_{12} f_e^{(0)} f_\mu^{(0)} \\ Y_{12} f_e^{(0)} f_\mu^{(0)} & Y_{22} f_\mu^{(0)2} \end{pmatrix}, \quad (24)$$

where we have assumed for simplicity a symmetric $5D$ Yukawa matrix. Assuming $\mathcal{O}(1)$ Yukawa couplings, the functional dependences of the fermion masses on the wave-functions are

$$m_e \sim f_e^{(0)2}, \quad m_\mu \sim f_\mu^{(0)2}, \quad (25)$$

while the mixing matrices take the form

$$U \sim \begin{pmatrix} 1 & -\sqrt{\frac{m_e}{m_\mu}} \\ \sqrt{\frac{m_e}{m_\mu}} & 1 \end{pmatrix}. \quad (26)$$

We therefore find that $|U_{12}| \sim \sqrt{\frac{m_e}{m_\mu}}$. Including the τ then gives $|U_{13}| \sim \sqrt{\frac{m_e}{m_\tau}}$ and $|U_{23}| \sim \sqrt{\frac{m_\mu}{m_\tau}}$. The diagonal entries $|U_{ii}| \sim 1$. We will assume mixing matrix elements of these approximate magnitudes in our analysis.

D. Operator Matching

We discuss in this subsection the formalism we will use to compare the RS predictions to the experimental measurements. Our presentation closely follows the discussion in [21]. Tri-lepton decays of the form $l \rightarrow l_1 \bar{l}_2 l_3$ and $\mu - e$ conversion are mediated by tree-level mixing with heavy gauge bosons and generate four-fermion interactions, while $l \rightarrow l' \gamma$ occurs via a loop-induced dipole operator. We can parameterize these effects in the following effective Lagrangian:

$$\begin{aligned} -\mathcal{L}_{\text{eff}} = & C_R(q^2) \frac{1}{2m_\mu} \bar{e}_R \sigma^{\mu\nu} F_{\mu\nu} \mu_L + C_L(q^2) \frac{1}{2m_\mu} \bar{e}_L \sigma^{\mu\nu} F_{\mu\nu} \mu_R \\ & + \frac{4G_F}{\sqrt{2}} [g_3 (\bar{e}_R \gamma^\mu \mu_R) (\bar{e}_R \gamma_\mu e_R) + g_4 (\bar{e}_L \gamma^\mu \mu_L) (\bar{e}_L \gamma_\mu e_L) \\ & + g_5 (\bar{e}_R \gamma^\mu \mu_R) (\bar{e}_L \gamma_\mu e_L) + g_6 (\bar{e}_L \gamma^\mu \mu_L) (\bar{e}_R \gamma_\mu e_R)] + \text{h.c.} \end{aligned} \quad (27)$$

The form factors¹ $C_{L,R}(q^2)$ and the couplings g_i are then computed in a straightforward matching procedure. We will discuss this computation in detail in the following two sections.

¹ Note that these form factors are normalized differently than the $A_{L,R}$ in [21]: $C = -\frac{8G_F m_\mu^2}{\sqrt{2}} A$.

III. TRI-LEPTON DECAYS AND $\mu - e$ CONVERSION

In this section and the next we study the predictions that the minimal RS model makes for lepton flavor violation. We focus on processes in the muon sector, such as $\mu^- \rightarrow e^+ e^- e^-$ and $\mu - e$ conversion in the presence of nuclei, and rare tau decays of the form $\tau \rightarrow l_1 \bar{l}_2 l_3$ currently being studied at BABAR and BELLE. The dipole-mediated decays will be discussed in the next section.

The dominant effects arise from flavor non-diagonal couplings of the zero-mode Z -boson. Contributions from exchange of the Higgs boson are suppressed by small fermion masses, and we will show later that those coming from direct KK exchange are suppressed by a large fermion wave-function factor. There are also contributions to these processes from the dipole exchanges denoted by $C_{L,R}$ in Eq. 27, but these are loop-suppressed and small in the parameter space of interest. We also find that KK -fermion mixing effects are sub-dominant in the parameter space of interest. We derive here the relevant couplings. We denote the physical basis by Z_0, Z_1 , and the gauge basis by $Z^{(0)}, Z^{(1)}$. For simplicity, we restrict our discussion here to the first KK level; in our analysis we include the first several modes. After diagonalizing the gauge boson mass matrix, we find that these are related via

$$Z^{(0)} = Z_0 + f \frac{m_Z^2}{M_{KK}^2} Z_1, \quad Z^{(1)} = Z_1 - f \frac{m_Z^2}{M_{KK}^2} Z_0. \quad (28)$$

f parameterizes the mixing between the zero and first KK level. With a brane Higgs field, $f = \sqrt{2k\pi r_c} \sim \mathcal{O}(10)$. A plot of f for a bulk Higgs field is shown in Fig. 1. The couplings between the zero-mode fermions and $Z^{(1)}$ are determined by the appropriate overlap integral. We define the ratio of these couplings to the SM couplings as α_e, α_μ , and α_τ , where $g^{(1)} = \alpha g^{SM}$; the α_i are then given by

$$\alpha_i = 2\sqrt{2\pi} \int_0^\pi d\phi e^\sigma \chi^{(1)} [f_i^{(0)}]^2. \quad (29)$$

Since the fermion wave-functions are localized at different points in the bulk, the α_i differ, but they are all roughly $\mathcal{O}(0.1)$ in magnitude. We present a plot of the α_i in Fig. 3. In the fermion flavor basis, the matrix which describes the $Z^{(1)}$ couplings takes the form

$$g^{SM} (\bar{e}_F, \bar{\mu}_F, \bar{\tau}_F) Z^{(1)} \begin{pmatrix} \alpha_e & 0 & 0 \\ 0 & \alpha_\mu & 0 \\ 0 & 0 & \alpha_\tau \end{pmatrix} \begin{pmatrix} e_F \\ \mu_F \\ \tau_F \end{pmatrix}. \quad (30)$$

We must first rotate the fermions to the mass basis. As was explained in the last section, we introduce unitary matrices U_L, U_R , so that $L_M = U_L L_F, R_M = U_R R_F$, where L_F denotes the left-handed flavor basis-vector, L_M the left-handed mass basis-vector, etc. The flavor-basis coupling matrices $C_{L,R}^F = g_{L,R} \text{diag}(\alpha_e, \alpha_\mu, \alpha_\tau)$ are rotated to $C_{L,R} = U_{L,R} C_{L,R}^F U_{L,R}^\dagger$. The flavor-violating couplings are the off-diagonal entries of $C_{L,R}$; we find

$$\begin{aligned} g_{L,R}^{(1)\mu e} &= g_{L,R} \left(U_{11}^{L,R} U_{21}^{L,R*} \alpha_e + U_{12}^{L,R} U_{22}^{L,R*} \alpha_\mu + U_{13}^{L,R} U_{23}^{L,R*} \alpha_\tau \right), \\ g_{L,R}^{(1)\tau\mu} &= g_{L,R} \left(U_{21}^{L,R} U_{31}^{L,R*} \alpha_e + U_{22}^{L,R} U_{32}^{L,R*} \alpha_\mu + U_{23}^{L,R} U_{33}^{L,R*} \alpha_\tau \right), \\ g_{L,R}^{(1)\tau e} &= g_{L,R} \left(U_{11}^{L,R} U_{31}^{L,R*} \alpha_e + U_{12}^{L,R} U_{32}^{L,R*} \alpha_\mu + U_{13}^{L,R} U_{33}^{L,R*} \alpha_\tau \right), \end{aligned} \quad (31)$$

where $g_{L,R}$ are the usual SM couplings. We can use the unitarity of $U_{L,R}$ to rewrite these as

$$\begin{aligned} g_{L,R}^{(1)\mu e} &= g_{L,R} \left[U_{12}^{L,R} U_{22}^{L,R*} (\alpha_\mu - \alpha_e) + U_{13}^{L,R} U_{23}^{L,R*} (\alpha_\tau - \alpha_e) \right], \\ g_{L,R}^{(1)\tau\mu} &= g_{L,R} \left[U_{21}^{L,R} U_{31}^{L,R*} (\alpha_e - \alpha_\mu) + U_{23}^{L,R} U_{33}^{L,R*} (\alpha_\tau - \alpha_\mu) \right], \\ g_{L,R}^{(1)\tau e} &= g_{L,R} \left[U_{12}^{L,R} U_{32}^{L,R*} (\alpha_\mu - \alpha_e) + U_{13}^{L,R} U_{33}^{L,R*} (\alpha_\tau - \alpha_e) \right]. \end{aligned} \quad (32)$$

Using Eq. 28, the couplings to Z_0 are obtained via multiplication by $-f m_Z^2 / M_{KK}^2$: $g_{L,R}^{\mu e} = -f m_Z^2 / M_{KK}^2 g_{L,R}^{(1)\mu e}$, etc. The couplings to Z_1 are identical to those in Eq. 32, to leading order in the gauge boson mixing.

We now use these to derive the flavor-violating couplings g_{3-6} of Eq. 27:

$$\begin{aligned} g_3^{\mu e} &= 2g_R \left[g_R^{\mu e} + \alpha_e g_R^{(1)\mu e} \frac{m_Z^2}{M_{KK}^2} \right], \\ g_4^{\mu e} &= 2g_L \left[g_L^{\mu e} + \alpha_e g_L^{(1)\mu e} \frac{m_Z^2}{M_{KK}^2} \right], \\ g_5^{\mu e} &= 2g_L \left[g_R^{\mu e} + \alpha_e g_R^{(1)\mu e} \frac{m_Z^2}{M_{KK}^2} \right], \\ g_6^{\mu e} &= 2g_R \left[g_L^{\mu e} + \alpha_e g_L^{(1)\mu e} \frac{m_Z^2}{M_{KK}^2} \right]. \end{aligned} \quad (33)$$

These are for $\mu - e$ flavor violation; similar expressions hold for $\tau - \mu$ and $\tau - e$. The first term on each line is from the Z_0 coupling, while the second is from direct Z_1 exchange. Substituting in the expressions from Eq. 32, we find

$$g_3^{\mu e} = -2g_R^2 \frac{m_Z^2}{M_{KK}^2} (f - \alpha_e) \left[U_{12}^R U_{22}^{R*} (\alpha_\mu - \alpha_e) + U_{13}^R U_{23}^{R*} (\alpha_\tau - \alpha_e) \right], \quad (34)$$

and similar expressions for the other couplings. Since $f \gg |\alpha_e|$, we can neglect the direct KK exchange effect.

We will study the decays $\mu^- \rightarrow e^- e^+ e^-$, $\tau^- \rightarrow \mu^- \mu^+ \mu^-$, $\tau^- \rightarrow e^- e^+ e^-$, $\tau \rightarrow \mu^- e^+ e^-$, and $\tau \rightarrow e^- \mu^+ e^-$. The remaining rare τ decays studied at BABAR and BELLE, $\tau \rightarrow e^- \mu^+ e^-$ and $\tau \rightarrow \mu^- e^+ \mu^-$, require an additional flavor-violating coupling than those above, and are therefore highly suppressed. The relevant branching fractions from [21] are

$$\begin{aligned} BR(\mu \rightarrow 3e) &= 2 (|g_3^{\mu e}|^2 + |g_4^{\mu e}|^2) + |g_5^{\mu e}|^2 + |g_6^{\mu e}|^2, \\ BR(\tau \rightarrow 3\mu) &= 2 (|g_3^{\tau\mu}|^2 + |g_4^{\tau\mu}|^2) + |g_5^{\tau\mu}|^2 + |g_6^{\tau\mu}|^2, \\ BR(\tau \rightarrow 3e) &= 2 (|g_3^{\tau e}|^2 + |g_4^{\tau e}|^2) + |g_5^{\tau e}|^2 + |g_6^{\tau e}|^2, \\ BR(\tau \rightarrow \mu e e) &= |g_3^{\tau\mu}|^2 + |g_4^{\tau\mu}|^2 + |g_5^{\tau\mu}|^2 + |g_6^{\tau\mu}|^2, \\ BR(\tau \rightarrow e \mu \mu) &= |g_3^{\tau e}|^2 + |g_4^{\tau e}|^2 + |g_5^{\tau e}|^2 + |g_6^{\tau e}|^2. \end{aligned} \quad (35)$$

The $\mu - e$ conversion rate is given by [22]

$$B_{conv} = \frac{2p_e E_e G_F^2 m_\mu^3 \alpha^3 Z_{eff}^4 Q_N^2}{\pi^2 Z \Gamma_{capt}} [|g_R^{\mu e}|^2 + |g_L^{\mu e}|^2], \quad (36)$$

where G_F is the Fermi constant, α is the QED coupling strength, and the remaining terms are atomic physics constants defined in [22]. Numerical values for titanium, for which the most sensitive limits have been obtained [23], can be found in [21].

We will present a detailed scan of the anarchic RS parameter space in a later section. For now, to provide some guidance as to what scales these rare decays can probe, we perform a few simple estimates. We set the 5-D fermion Yukawas to the values suggested by 5-D Yukawa anarchy, $Y_e = Y_\mu = Y_\tau = 2$. We also use the intuition described in the previous section to set the mixing matrix entries to the values

$$U_{11}^{L,R} = 1, \quad U_{12}^{L,R} = \sqrt{\frac{m_e}{m_\mu}}, \quad U_{13}^{L,R} = \sqrt{\frac{m_e}{m_\tau}}, \quad (37)$$

and similarly for the remaining rows of $U_{L,R}$; for this estimate, we set the phases of these elements to zero. We choose a value of $kr_c = 11.27$. We include the first 3 KK modes in this estimate, and we have checked that adding more does not affect our results. Employing these approximations, we check what limits can be obtained on M_{KK} from each process. We impose the following bounds: $BR(\mu \rightarrow 3e) < 10^{-12}$, which is the current PDG limit [24]; $B_{conv} < 6.1 \times 10^{-13}$, which is the strongest constraint obtained by the experiment SINDRUM II [23]. For the rare tau decays, we employ the strongest constraints from either BABAR or BELLE, which are $BR(\tau \rightarrow l_1 \bar{l}_2 l_3) < 2 \times 10^{-7}$ for each mode [25]. We present the bounds on M_{KK} for both the brane Higgs model and the bulk Higgs scenario with $\nu = 0$ in Table I. The limits from $BR(\mu \rightarrow 3e)$ and B_{conv} already probe the multi-TeV region, similar to that

	Brane Higgs	$\nu = 0$
$BR(\mu \rightarrow 3e)$	2.5 TeV	2.0 TeV
B_{conv}	5.9	4.7
$BR(\tau \rightarrow 3\mu)$	0.62	0.51
$BR(\tau \rightarrow \mu ee)$	0.55	0.46
$BR(\tau \rightarrow 3e)$	0.16	0.13
$BR(\tau \rightarrow e\mu\mu)$	0.14	0.12

TABLE I: Constraints on the first KK mode mass, M_{KK} , coming from various measurements for both a brane Higgs field and for the bulk Higgs case with $\nu = 0$. The bounds on M_{KK} are in TeV.

possible at the LHC. Although the limits from rare τ -decays are lower, they probe different model parameters which describe the third generation. These bounds will also improve as the B -factories acquire more data. We will show that these bounds are generic throughout the entire parameter space in a later section.

IV. DIPOLE OPERATOR MEDIATED DECAYS

We now compute the decays of the form $l \rightarrow l' \gamma$, which are induced at the loop level by the diagram shown in Fig. 2. For simplicity, we discuss the decay $\mu \rightarrow e \gamma$. It is simple to translate our expressions into results for τ decays. The dominant contributions to these amplitudes come from exchange of a Higgs boson and KK fermions. This is because these diagrams contain terms proportional to the fourth power of the fermion wave-function ratio

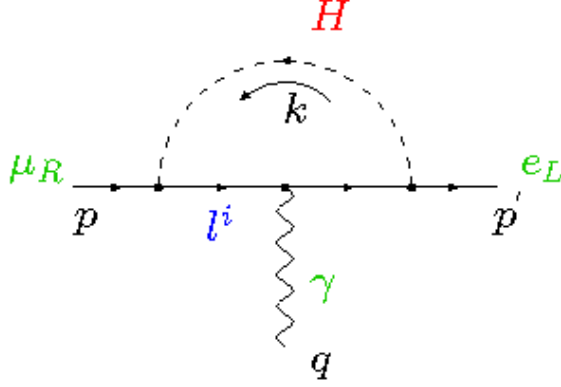


FIG. 2: The Feynman diagram generating the dipole operator which mediates $l \rightarrow l' \gamma$ decays. l^i are the physical KK leptons. We have specialized to $\mu \rightarrow e \gamma$ in the figure. There is a similar diagram with $L \leftrightarrow R$.

$f_{e,\mu} = f_{e,\mu}^{(1)}/f_{e,\mu}^{(0)}$. For $c = 1/2$, this ratio is $f_{e,\mu} = 2\pi k r_c \approx 70$; it grows rapidly for $c > 1/2$, the values relevant for the muon and the electron. This strong dependence on the fermion wave-function was first noted in [26]. There are also contributions coming from loops of KK Z bosons and KK fermions. However, as argued in reference [11] for the case of the KK gluon contribution to radiative quark decays, the flavor structure of this diagram is approximately aligned with the $4D$ Yukawa matrix and hence gives a suppressed contribution. The KK fermion-Higgs diagrams have a different flavor structure than the $4D$ Yukawa matrix.

The amplitude for the diagram in Fig. 2 is

$$\begin{aligned}
A(\mu \rightarrow e \gamma) &= \sum_i \int \frac{d^4 k}{(2\pi)^4} \bar{u}(p') (i\Lambda_{e^0 i}) \frac{i(\not{p}' + M_{KK}^{(i)})}{\hat{p}'^2 - M_{KK}^{(i),2}} (ie\gamma^\mu A_\mu) \frac{i(\not{p} + M_{KK}^{(i)})}{\hat{p}^2 - M_{KK}^{(i),2}} (i\Lambda_{i\mu^0}) u(p) \cdot \frac{i}{k^2 - m_H^2} \\
&= \bar{u}(p') \left[-e A_\mu \sum_i \Lambda_{e^0 i} \int \frac{d^4 k}{(2\pi)^4} \frac{(\not{p}' + M_{KK}^{(i)}) \gamma^\mu (\not{p} + M_{KK}^{(i)})}{(\hat{p}'^2 - M_{KK}^{(i),2})(\hat{p}^2 - M_{KK}^{(i),2})(k^2 - m_H^2)} \Lambda_{i\mu^0} \right] u(p), \quad (38)
\end{aligned}$$

where $\hat{p}^{(\prime)} = p^{(\prime)} + k$ and Λ_{ij} are the Yukawa matrices. We will assume the external lines are massless, which is valid up to subleading corrections in $1/f_{e,\mu}$. We have denoted the KK fermion masses by $M_{KK}^{(i)}$. At each KK level, there are two vector-like fermion pairs for each flavor with masses $M_{KK}^{(1)}$ and $M_{KK}^{(2)}$, as is clear from Eq. 6. The splitting of these masses through mixing will be important in evaluating this contribution. It is straightforward to evaluate this integral to find

$$A(\mu \rightarrow e \gamma; q^2) = \frac{1}{2m_\mu} \bar{u}(p') \sigma^{\mu\nu} F_{\mu\nu} u(p) \times (-i)C(q^2), \quad (39)$$

where

$$-iC(q^2) = \frac{iem_\mu}{16\pi^2} \sum_i \Lambda_{e^0 i} \left\{ \int_0^1 dz \int_0^{1-z} dy \frac{M_{KK}^{(i)}(1-z)}{q^2 y(1-y-z) - (1-z)M_{KK}^{(i),2} - zm_H^2} \right\} \Lambda_{i\mu^0}. \quad (40)$$

We now set $q^2 = 0$ to derive

$$C(q^2 = 0) = \frac{em_\mu}{32\pi^2} \sum_i \Lambda_{e^0 i} \frac{I(m_H^2/M_{KK}^{(i),2})}{M_{KK}^{(i)}} \Lambda_{i\mu^0}, \quad (41)$$

where $I(x) = 1 - x + \mathcal{O}(x^2)$. The branching fraction becomes [21]

$$B(\mu \rightarrow e\gamma) = \frac{12\pi^2}{(G_F m_\mu^2)^2} [|C_L(0)|^2 + |C_R(0)|^2], \quad (42)$$

where we have inserted the helicity labels L, R on C . These helicity labels dictate which elements of the Yukawa matrix Λ should be used; we will make this explicit in the following discussion. We now consider separately the brane and bulk Higgs field cases. We will find that the brane Higgs prediction for $l \rightarrow l' \gamma$ is not calculable because it is sensitive to cut-off scale physics, while for the bulk Higgs case we can use our 5D effective field theory to make robust predictions.

A. UV sensitivity for the case of brane Higgs field

The leading contribution in Eq. 41, with $m_H = 0$ and $I(x) = 1$, vanishes up to factors suppressed by $1/f^2$ for a brane Higgs field because of the Yukawa matrix structure. With $m_H = 0$, we are only considering contributions proportional to $1/M_{KK}^{(1,2)}$. This mass splitting is cancelled by shifts in the Yukawa couplings to all orders in v/M_{KK} . The leading result therefore comes from $1/(M_{KK}^{(1,2)})^3$ contributions, and we must consider the m_H^2 terms to obtain these. The diagonalization of the fermion mass matrix in Eq. 14 is discussed in the detail in the Appendix. The result of this analysis is the following mass splitting:

$$\frac{1}{(M_{KK}^{(1)})^3} - \frac{1}{(M_{KK}^{(2)})^3} = -\frac{3\Delta_1}{M_{KK}^4}. \quad (43)$$

This yields the following coefficients of the dipole operator:

$$\begin{aligned} C_L(0) &= \frac{em_\mu m_H^2}{32\pi^2 M_{KK}^4} [\Delta_R \Delta_1 \Delta_L]_{e\mu}, \\ C_R(0) &= \frac{em_\mu m_H^2}{32\pi^2 M_{KK}^4} [\Delta_R \Delta_1 \Delta_L]_{e\mu}^\dagger. \end{aligned} \quad (44)$$

The Yukawa structures entering C_L and C_R differ by a hermitian conjugate.

However, it turns out that this result is masked by cut-off effects. A similar ultraviolet sensitivity of Higgs-fermion KK loops was also noted in [11]. The expected one-loop contribution from a given set of KK modes is finite with size

$$\frac{C_{L,R}^{KK}}{m_\mu^2} \sim \frac{\lambda_{5D}^2}{16\pi^2} \frac{1}{M_{KK}^2}. \quad (45)$$

For simplicity, we have not included the relevant mixing matrix elements in this estimate. Although the actual one-loop result for a brane Higgs field vanishes for $m_H = 0$, we cannot

find a symmetry that requires this, and we expect it to be an accident of the one-loop result. The sum over two independent KK modes would have given a logarithmic divergence at one-loop:

$$\frac{C_{L,R}^{KK}}{m_\mu^2} \propto \log N_{KK} \sim \log(\Lambda_{5D}/k) \sim \log(\tilde{\Lambda}_{5D}/M_{KK}). \quad (46)$$

Here, N_{KK} is the total number of KK modes in the 5D effective theory, Λ_{5D} is the 5D cut-off of order 10^{19} GeV, and $\tilde{\Lambda}_{5D}$ is the warped-down 5D cut-off of order TeV. Similarly, M_{KK} is roughly the warped-down curvature scale k . To obtain this logarithmic divergence, it is crucial that KK fermion-Higgs couplings in the sum are independent of the KK index. We expect that higher-loop contributions are strongly power divergent because of the increasing number of sums over KK modes, and are as important as the one-loop result provided the cut-off scale physics is strongly coupled.

This divergence structure can be more easily seen using power-counting in the 5D theory. Since the 5D Yukawa coupling has mass dimension $[\lambda_{5D}/k] = [-1]$, the loop expansion for $\mu \rightarrow e\gamma$ has the form

$$\frac{C_{L,R}^{KK}}{m_\mu^2} \sim \frac{1}{16\pi^2} \left(\frac{\lambda_{5D}}{M_{KK}} \right)^2 \left[\log \left(\frac{\Lambda_{5D}}{k} \right) + \frac{1}{16\pi^2} \frac{\lambda_{5D}^2}{k^2} \Lambda_{5D}^2 + \dots \right]. \quad (47)$$

In this expression, we have replaced the scale $k \sim 10^{18}$ GeV by its warped-down value M_{KK} in the overall coefficient. By simple dimensional analysis, the one-loop contribution can be log-divergent and the two-loop contribution is quadratically divergent; in KK language, the power divergence at two loops can be seen from the independent sums over 4 KK modes. The two-loop result is comparable to the one-loop prediction if the cut-off physics is strongly-coupled: $\Lambda_{5D}^2/k^2 \times \lambda_{5D}^2/(16\pi^2) \sim 1$. Therefore, the KK loop contribution is not calculable in this case.

Based on the above discussion, we also expect the higher-dimensional operators in the 5D theory coming from physics at the cut-off scale to be important. The relation between the warped-down 5D cut-off in the Yukawa sector and the KK scale for a brane Higgs field is $\tilde{\Lambda}_{5D} \sim M_{KK}/(4\pi/\lambda_{5D})$, based on power counting of the 5D loop factor. To obtain the cut-off operator, we replace M_{KK} in Eq. 45 by the cut-off scale $\tilde{\Lambda}_{5D}$, and the loop factor by ~ 1 , since the cut-off effect has no loop suppression. This shows that $\mu \rightarrow e\gamma$ is an UV sensitive observable for a Higgs field on the TeV brane. We can only parameterize the contribution as:

$$C_{L,R}^{total} = a \frac{m_\mu^2}{\tilde{\Lambda}_{5D}^2} \times U_{12}^{L,R}, \quad (48)$$

where a is an unknown, $O(1)$ coefficient, and we have included the appropriate mixing matrix element.

We now show that we can reliably calculate dipole induced decays for a bulk Higgs field. The Yukawa coupling in this case has mass dimension $[\lambda_{5D}/\sqrt{k}] = [-1/2]$, so the loop expansion is instead

$$\frac{C_{L,R}^{KK}}{m_\mu^2} \sim \frac{1}{16\pi^2} \left(\frac{\lambda_{5D}}{\sqrt{M_{KK}}} \right)^2 \left[\frac{1}{M_{KK}} + \frac{1}{16\pi^2} \frac{\lambda_{5D}^2}{M_{KK}} \log \left(\frac{\Lambda_{5D}}{k} \right) + \left(\frac{1}{16\pi^2} \right)^2 \frac{\lambda_{5D}^4}{M_{KK}^2} \tilde{\Lambda}_{5D} + \dots \right].$$

From this 5D power-counting, we see that the one-loop KK contribution is finite. The two-loop result is logarithmically divergent, but is smaller than the one-loop prediction by ~ 0.1

provided $\lambda_{5D} \lesssim 4$. Three-loop and higher contributions are power-divergent and comparable to the two-loop result, but are again smaller than the one-loop effect.

Thus, in the bulk Higgs case, the KK effect is calculable. The effects from cut-off scale operators are suppressed, and we can reliably make a prediction using the RS theory. In our numerical analysis, we will include dipole decays for the bulk Higgs field case. For the brane Higgs scenario we will simply neglect them, since we cannot make a reliable prediction.

B. Contributions from a bulk Higgs field

We now consider the scenario when the Higgs boson is allowed to propagate in the bulk. In this case, the KK mode result is not overwhelmed by cut-off scale operators. The $m_H = 0$ limit does not vanish for a bulk Higgs. We make this approximation in our discussion, since the corrections are $\mathcal{O}(m_H^2/M_{KK}^2)$. We first work out the Yukawa structure appearing in Eq. 41. Using the results in the Appendix for the two KK fermions appearing in the diagram of Fig. 2, we find

$$\begin{aligned} (\bar{e}_L^0 l_R^1)(\bar{l}_L^1 \mu_R^0) &= \left[\Delta_R \left[1 + \left(\frac{X}{4} - \frac{\Delta_2}{M_{KK}} \right) \right] \right]_{el} \left(\frac{1}{M_{KK}^{(1)}} \right) \left[\left[1 + \left(\frac{X}{4} - \frac{\Delta_2}{M_{KK}} \right) \right] \Delta_L \right]_{l\mu} \\ (\bar{e}_L^0 l_R^2)(\bar{l}_L^2 \mu_R^0) &= \left[\Delta_R \left[1 - \left(\frac{X}{4} - \frac{\Delta_2}{M_{KK}} \right) \right] \right]_{el} \left(-\frac{1}{M_{KK}^{(2)}} \right) \left[\left[1 - \left(\frac{X}{4} - \frac{\Delta_2}{M_{KK}} \right) \right] \Delta_L \right]_{l\mu} \end{aligned} \quad (49)$$

In this expression we must sum over $l = e, \mu, \tau$. To simplify this we use the splitting between the KK fermion masses derived in the Appendix:

$$\frac{1}{M_{KK}^{(1)}} - \frac{1}{M_{KK}^{(2)}} = -\frac{\Delta_1 + \Delta_2}{M_{kk}^2} + \mathcal{O}\left(\frac{v^3}{M_{kk}^4}\right). \quad (50)$$

We find the following results for the dipole operator coefficients:

$$\begin{aligned} C_L(0) &= \frac{3em_\mu}{32\pi^2 M_{KK}^2} [\Delta_R \Delta_2 \Delta_L]_{e\mu} \\ C_R(0) &= \frac{3em_\mu}{32\pi^2 M_{KK}^2} [\Delta_R \Delta_2 \Delta_L]_{e\mu}^\dagger \end{aligned} \quad (51)$$

We note that in the limit of the Higgs boson being localized on the TeV brane, $\Delta_2 \rightarrow 0$; the result vanishes in this limit, as required.

An identical analysis can be performed for $\tau \rightarrow \mu\gamma$ and $\tau \rightarrow e\gamma$. We simply replace $m_\mu \rightarrow m_\tau$ and change the indices of the Yukawa structure appropriately in Eq. 51. We now perform an estimate of the bounds similar to that performed in the brane Higgs case. We set $Y_e = Y_\mu = Y_\tau = 2$, and set the mixing matrix elements to their canonical values as described before. We also set $\nu = 0$. We impose the following bounds on each of the three dipole decays: $BR(\mu \rightarrow e\gamma) < 1.2 \times 10^{-11}$, as obtained from [24]; $BR(\tau \rightarrow \mu\gamma) < 9 \times 10^{-8}$, the stronger of the bounds coming from BABAR and BELLE [27]; $BR(\tau \rightarrow e\gamma) < 1.1 \times 10^{-7}$, again the stronger of the bounds coming from BABAR and BELLE [28]. We find the following constraints for the canonical parameters:

$$\begin{aligned} BR(\mu \rightarrow e\gamma) &: M_{KK} > 15.8 \text{ TeV}; \\ BR(\tau \rightarrow e\gamma) &: M_{KK} > 1.4 \text{ TeV}; \\ BR(\tau \rightarrow \mu\gamma) &: M_{KK} > 2.4 \text{ TeV}. \end{aligned} \quad (52)$$

The constraints, particularly from $BR(\mu \rightarrow e\gamma)$, are quite strong. This arises in part from the large value of the Yukawa coupling, $Y = 2$, as we now discuss.

C. Tension between tree-level and loop-induced processes

We now discuss a tension between processes caused by tree-level gauge boson mixing such as $\mu - e$ conversion and $l \rightarrow l_1 \bar{l}_2 l_3$, and dipole operator decays. These have opposite dependences on the $5D$ Yukawa couplings, leading to strong constraints for all parameter choices. We first give a very simple scaling argument to motivate this, and then present numerical proof.

Our scaling argument uses the dependence of each process on the zero-mode fermion wave-function $f_l^{(0)}$ evaluated at the TeV brane. We will work for simplicity in the large ν limit, which mimics a brane-localized Higgs field. From Eqs. 22 and 23, we find that the wave-function scales roughly as $f_l^{(0)} \sim 1/\sqrt{\lambda_{5D}}$. The wave-function has weak c -dependent factors which we will ignore in this argument. The quantity that governs the flavor violation in gauge boson mixing is the difference between α_l 's, as is clear from Eq. 34. In the definition of α_l in Eq. 29, we can divide the overlap integral into two regions, one near the Planck brane and the other near the TeV brane, to show that the former is c -independent and that the latter carries the c -dependence and must be $\alpha_l|_{non-universal} \sim [f_l^{(0)}]_{TeVbrane}^2 \sim 1/\lambda_{5D}$. We therefore expect the non-universal part of α_l , and hence the flavor violation, to decrease for larger Yukawa couplings, which is indeed what we observe in Fig. 3. For the dipole mediated decays, recall that in Section IV we claimed that the operator coefficients $C_{L,R}$ scaled as $C_{L,R} \sim 1/[f_l^{(0)}]^4 \sim \lambda_{5D}^2$; this can be verified using Eq. 51 and the results in the Appendix. The constraints coming from $l \rightarrow l' \gamma$ decays will increase with larger Yukawa couplings, the opposite dependence of the tree-level processes.

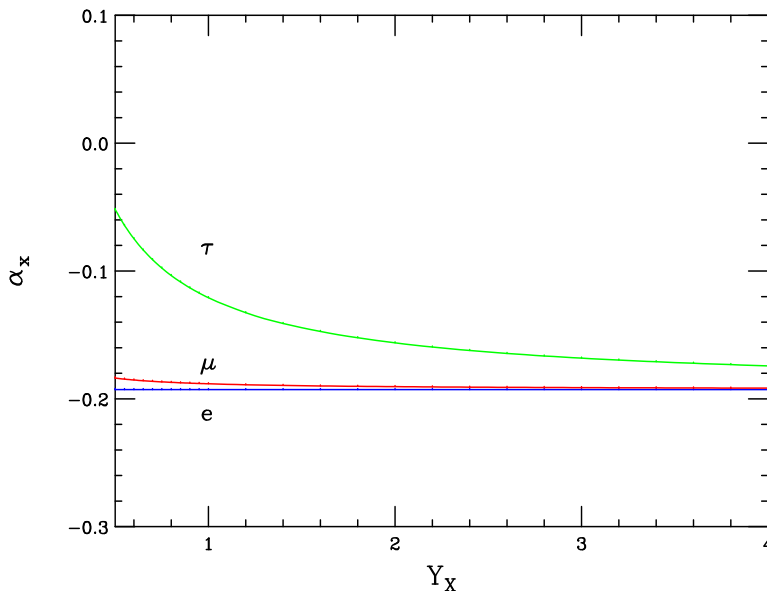


FIG. 3: The ratios of the zero-mode fermion couplings to $Z^{(1)}$ over their SM values, for $x = e, \mu, \tau$, as functions of the Yukawa couplings Y_x .

To exhibit this behavior we present in Table II the bounds on the first KK mode mass for

canonical mixing angles, $\nu = 0$, and for the two choices of Yukawa strength $Y_e = Y_\mu = Y_\tau = 1, 2$. We show the two most constraining processes, $\mu - e$ conversion and $BR(\mu \rightarrow e\gamma)$. The dependence on the Yukawa couplings agrees with our simple estimate above. We will find in the next section that this leads to strong constraint throughout the entire model parameter space.

	$Y = 1$	$Y = 2$
B_{conv}	6.7 TeV	4.7 TeV
$BR(\mu \rightarrow e\gamma)$	8.0	15.8

TABLE II: Constraints on the first KK mode mass, M_{KK} , coming from $\mu - e$ conversion and $BR(\mu \rightarrow e\gamma)$, for canonical mixing angles, $\nu = 0$, and for $Y = 1, 2$.

V. MONTE-CARLO SCAN OF THE ANARCHIC RS PARAMETER SPACE

In this section we present our Monte-Carlo scan of the RS parameter space, to determine in detail how well the RS geometric origin of flavor can be tested by current and future lepton flavor-violation experiments.

We first describe the ranges over which we scan the various RS parameters. The scenario introduced in the previous sections contains the following free parameters: Y_e, Y_μ, Y_τ , the overall Yukawa couplings for the electron, muon, and tau; $U_{ij}^{L,R}$, the elements of both the left and right-handed mixing matrices; the KK mass M_{KK} . We make the following assumptions in our scan.

- We restrict the Yukawa couplings to the range $Y_x \in [\frac{1}{2}, 4]$. As discussed before, the natural value is $Y_x \approx 2$. Values larger than 4 begin to invalidate the perturbative expansion, while values smaller than 1/2 introduce an unnatural hierarchy in the model. We explained in the previous section that flavor violation cannot be removed by making the Yukawa couplings either large or small, due to tension between tree-level and loop-induced processes.
- We implement the anarchy of 5-D couplings in our scan, which indicates that $U_{ii}^{L,R} \sim 1$, $U_{12}^{L,R} \sim \sqrt{m_e/m_\mu}$, $U_{13}^{L,R} \sim \sqrt{m_e/m_\tau}$, etc. We fix $U_{ii}^{L,R} = 1$, and define the canonical values

$$U_{12}^c = \sqrt{\frac{m_e}{m_\mu}}, \quad U_{13}^c = \sqrt{\frac{m_e}{m_\tau}}, \quad U_{23}^c = \sqrt{\frac{m_\mu}{m_\tau}}. \quad (53)$$

We then vary $U_{12}^L = \beta_{12}^L U_{12}^c$, with $\beta_{12}^L \in [1/4, 4]$. We independently vary $U_{12}^R, U_{13}^{L,R}$, and $U_{23}^{L,R}$ in a similar fashion. Again, we restrict the values to these ranges to insure no unnatural hierarchies in model parameters. We generate phases for the six independent $U^{L,R}$ in the range $[0, 2\pi]$.

- We approximately implement unitarity of the mixing matrices by setting $U_{21}^{L,R} = -(U_{12}^{L,R})^*$, etc. This assures that unitarity is maintained up to corrections of the level $\sqrt{m_e/m_\mu}, \sqrt{m_\mu/m_\tau}$, which is sufficient for the scan performed here.

We scan over the following fifteen independent parameters: the three Y_x , and the six complex mixing matrix elements $U_{12}^{L,R}$, $U_{13}^{L,R}$, and $U_{23}^{L,R}$. We generate 1000 sets of fifteen random numbers, and distribute them in the ranges indicated above for fixed M_{KK} . We perform two separate scans, one for a brane Higgs field and one for a bulk Higgs with $\nu = 0$. The ν dependence of the bulk Higgs field bounds is studied separately.

A. Scan for the brane Higgs field scenario

We first perform a Monte-Carlo scan of the parameter space of the brane Higgs scenario. As discussed in Section IV, dipole decays of the form $l \rightarrow l' \gamma$ are UV sensitive. We do not consider these decays in the brane Higgs case, which leaves us with $\mu - e$ conversion, $\mu \rightarrow 3e$, and $\tau \rightarrow l_1 \bar{l}_2 l_3$.

We first study the muonic processes $\mu \rightarrow 3e$ and $\mu - e$ conversion. We show in Fig. 4 scatter plots of the predictions for $BR(\mu \rightarrow 3e)$ and B_{conv} coming from our scan of the RS parameter space, for the KK scales $M_{KK} = 3, 5, 10$ TeV. The most sensitive probe is the SINDRUM II limit of $B_{conv} < 6.1 \times 10^{-13}$ [23]. This rules out a large fraction of the parameter space for $M_{KK} < 5$ TeV, and restricts the allowed parameters even at 10 TeV. The PDG limit of $BR(\mu \rightarrow 3e) < 10^{-12}$ is less severe: although it rules out a large fraction of the $M_{KK} = 3$ TeV parameter space, most of the $M_{KK} = 5$ TeV space is still allowed. We note there is an almost perfect correlation between the RS predictions for the two processes. This is not surprising; it is clear from Eqs. 35 and 36 that they depend almost identically on the same mixing angles.

This result has implications for both the aesthetic appeal of the anarchic RS flavor picture, and the observation of this physics at the LHC. Although points with $M_{KK} \leq 3$ TeV are still allowed, it is clear from Fig. 4 that the model as formulated in our scan prefers KK masses of 5 TeV or larger. Increasing the KK scale to these higher values introduces a large fine-tuning in the electroweak symmetry breaking sector and is therefore not favored [14, 16]. With such large KK masses, many associated states will also be too heavy to observe at the LHC. The other method of avoiding these constraints, reducing the $U_{ij}^{L,R}$ matrix elements to the appropriate level, implies either some additional structure or fine-tuning in the 5-D Yukawa matrix. We have studied the minimal model here, and it seems likely that more structure in the 5-D Yukawa matrix is needed for a completely natural description of the first and second generation flavor pattern in the brane Higgs case.

Another sector of the RS flavor picture to explore is that involving the third generation τ . This tests different model parameters than the muonic processes. We show in Fig. 5 a scatter plot of the RS predictions for $BR(\tau \rightarrow 3e)$ and $BR(\tau \rightarrow 3\mu)$ for $M_{KK} = 1$ TeV, together with the best limits coming from BABAR and BELLE. The lowest KK -scale allowed by electroweak precision tests in anarchic RS models is typically a few TeV. The B -factories are beginning to probe this region in the mode $\tau \rightarrow 3\mu$. There are plans to build a super- B factory with an integrated luminosity approaching 10 ab^{-1} [29]. The projected limits from this experiment are included in Fig. 5. Both the $\tau \rightarrow 3\mu$ and $\tau \rightarrow 3e$ modes at a super- B factory will constrain the anarchic RS parameter space. The LHC also has sensitivity to rare τ decays [30]; however, the projected sensitivities are slightly weaker than the current B -factory constraints, and have not been included. The expected sensitivities to rare τ decays at a future linear collider are also weaker than the limits set by the B -factories. Although the $M_{KK} \sim 1$ TeV scales probed with $\tau \rightarrow l_1 \bar{l}_2 l_3$ decays are lower than those constrained by $\mu - e$ conversion and $\mu \rightarrow 3e$, we stress that different model parameters are tested by each

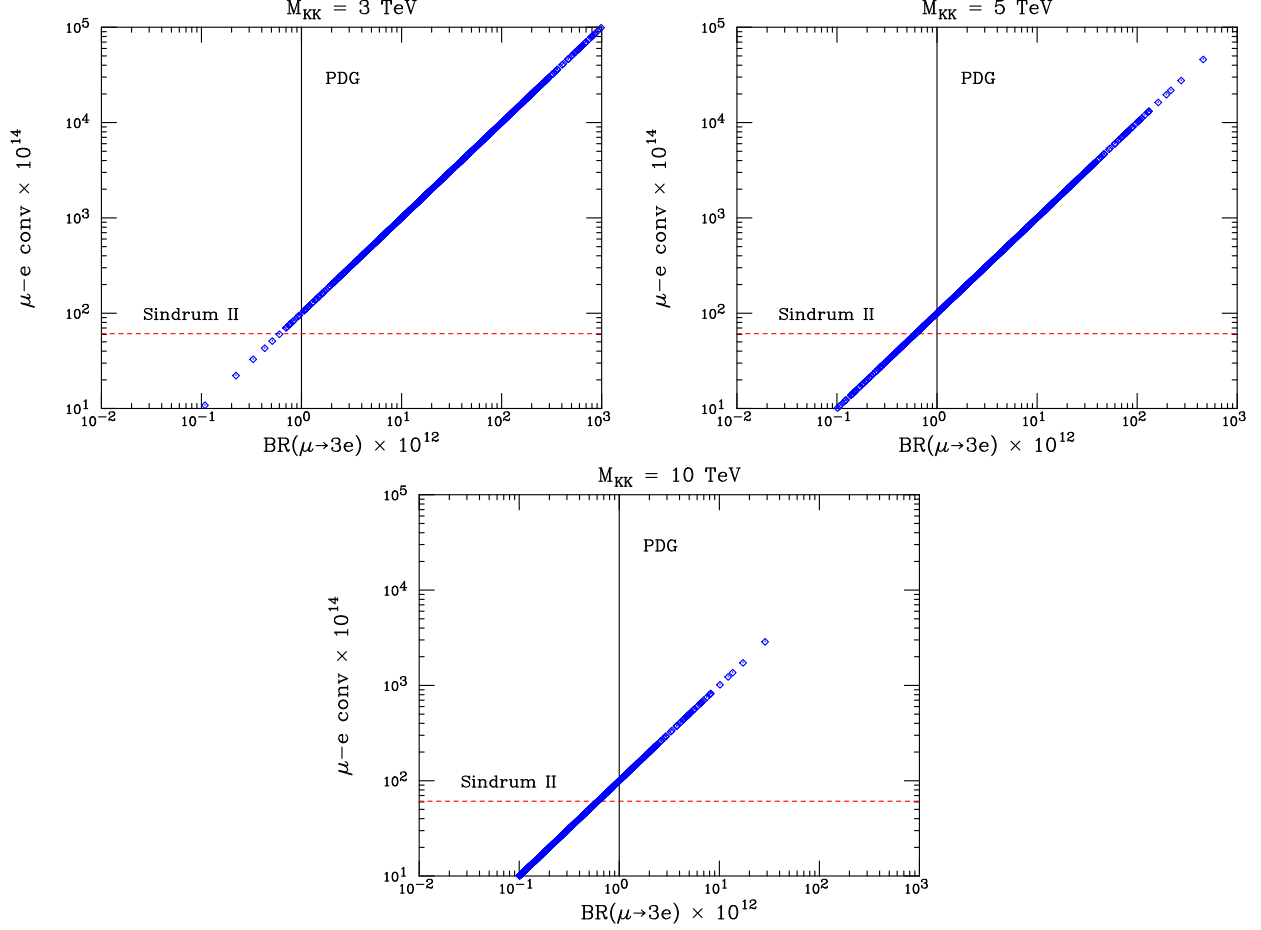


FIG. 4: Scan of the $\mu \rightarrow 3e$ and $\mu - e$ conversion predictions for $M_{KK} = 3, 5, 10$ TeV. The solid and dashed lines are the PDG and SINDRUM II limits, respectively.

set of processes.

B. Scan for the bulk Higgs field scenario

We now present the results of our scan over the bulk Higgs parameter space. For the scan we set $\nu = 0$, which mimics the composite (or A_5) Higgs model of [16]; we present separately the ν dependence of the most important constraints.

We again begin by considering muon initiated processes. The constraints from $\mu \rightarrow 3e$ and $\mu - e$ conversion are highly correlated, as we saw in the previous subsection. Since the bounds from $\mu - e$ conversion are stronger, we focus on this and $\mu \rightarrow e\gamma$. We show in Fig. 6 scatter plots of the predictions for $BR(\mu \rightarrow e\gamma)$ and B_{conv} coming from our scan of the RS parameter space, for the KK scales $M_{KK} = 3, 5, 10$ TeV. For $\mu \rightarrow e\gamma$ we include both the current constraint from the Particle Data Group [24] and the projected sensitivity of MEG [18]. The current bounds from $\mu \rightarrow e\gamma$ are quite strong; from the $M_{KK} = 3$ TeV plot in Fig. 6, we see that only one parameter choice satisfies the $BR(\mu \rightarrow e\gamma)$ bound. This point does not satisfy the $\mu - e$ conversion constraint. We can estimate that it would satisfy both bounds for $M_{KK} > 3.1$ TeV. In our scan over 1000 sets of model parameters the absolute lowest scale allowed is thus slightly larger than 3 TeV. Also, a large portion of

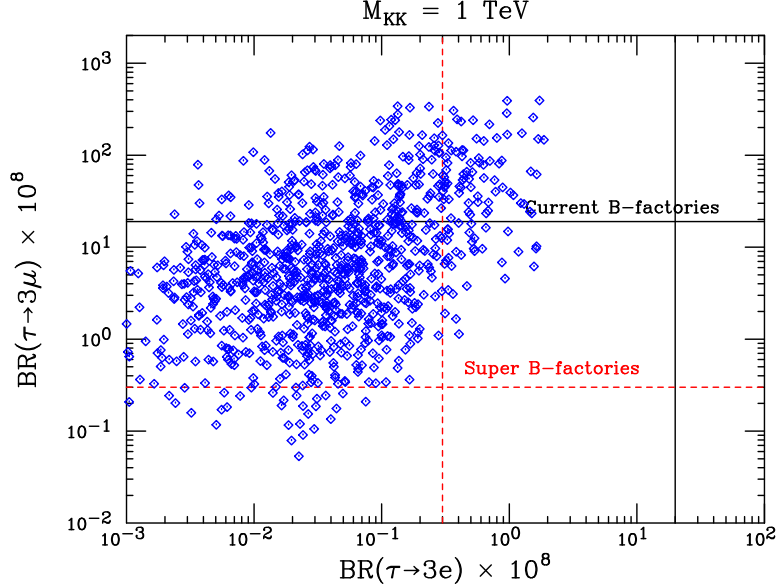


FIG. 5: Scan of the $\tau \rightarrow 3e$ and $\tau \rightarrow 3\mu$ predictions for $M_{KK} = 1$ TeV. The solid and dashed lines are the current B -factory and projected super- B factory limits, respectively.

the parameter set at both 5 and 10 TeV conflict with these bounds. We again find the need for a KK scale of $M_{KK} \geq 5$ TeV or additional structure in the mixing between the first and second generations to satisfy the experimental constraints for a significant fraction of model parameter space. In Fig. 7 we present the anarchic RS predictions for $\tau \rightarrow \mu\gamma$ and $\tau \rightarrow e\gamma$, together with current and future B -factory constraints, for $M_{KK} = 3$ TeV. The $\tau \rightarrow \mu\gamma$ mode is currently probing the few TeV range, while $\tau \rightarrow e\gamma$ will begin to test the anarchic RS scenario during the running of a super- B factory.

To study the sensitivity of the bulk Higgs field scenario to the location of the Higgs boson in the fifth dimension, we show in Fig. 8 the dependence of the $\mu - e$ conversion rate and $BR(\mu \rightarrow e\gamma)$ on ν . We set the mixing angles to their canonical values, and show results for $Y_x = 1, 2$ and $M_{KK} = 5, 10$ TeV. The $\mu - e$ conversion results are weakest for $\nu = 0$, and quickly asymptote to the brane Higgs result as ν becomes large. The variation of $\mu \rightarrow e\gamma$ with ν is more intricate. The vanishing of the calculable component of this process as the Higgs boson is moved towards the TeV brane, discussed in Section IV, is clearly seen in Fig. 8. However, we expect cut-off effects to become more important for large ν . There is a strong dependence of the process on the position of the Higgs field for small ν , with the result varying by an order of magnitude for $0 \leq \nu \leq 5$. The $\nu = 0$ case is again the most favorable choice. Since UV sensitivity of the model is reduced for a bulk Higgs field, and since the experimental constraints are weakest for $\nu = 0$, we conclude that there is a preference for models of the type presented in [16].

C. Future sensitivities of MEG and PRIME

Finally, we emphasize here the importance of future searches for $\mu - e$ conversion by PRIME and $\mu \rightarrow e\gamma$ by MEG. Our analysis has shown that with some small tuning of parameters, particularly for those describing the mixing of the first and second generation, KK scales of 3 TeV are allowed by current measurements. Alternatively, KK scales of 5

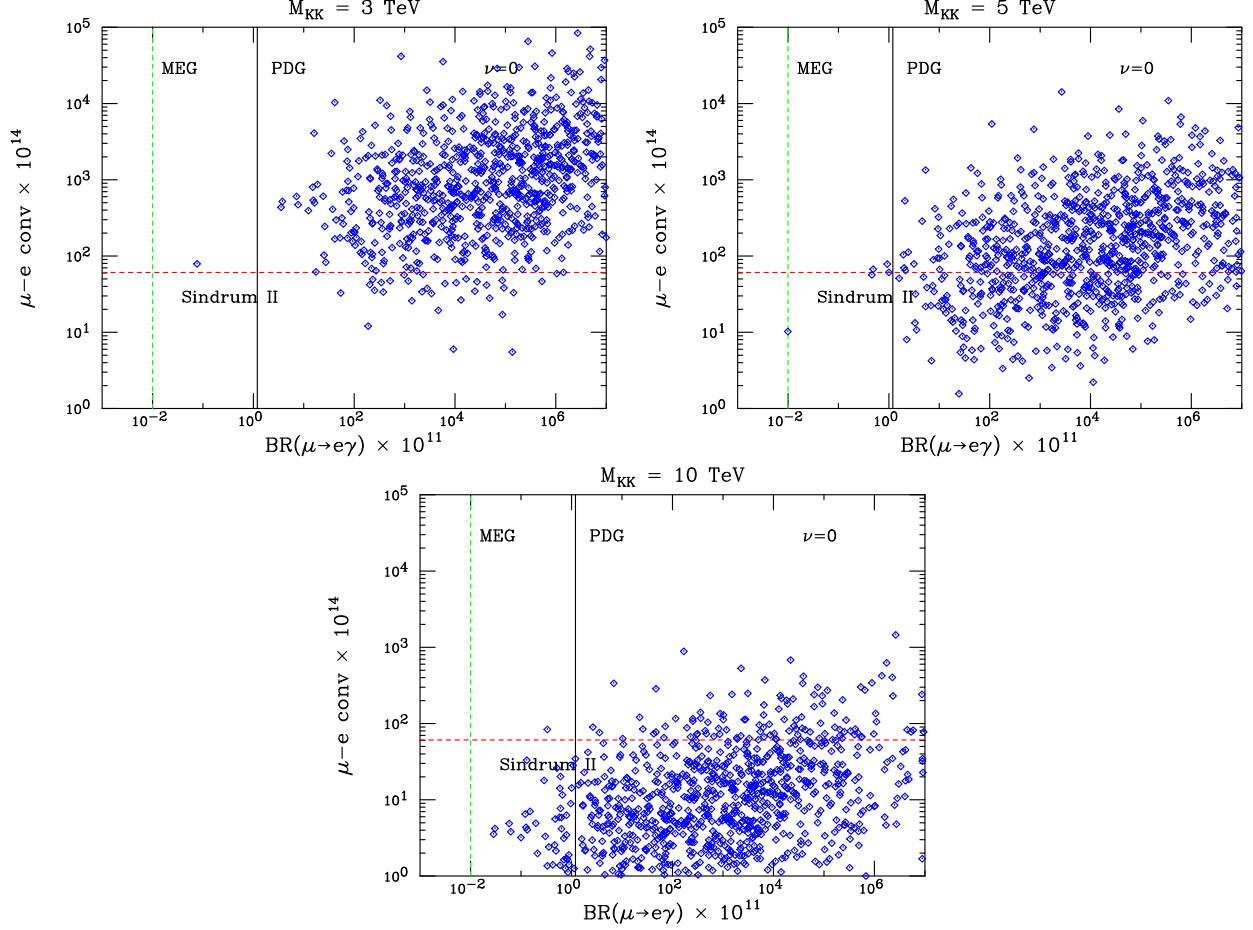


FIG. 6: Scan of the $\mu \rightarrow e\gamma$ and $\mu-e$ conversion predictions for $M_{KK} = 3, 5, 10$ TeV and $\nu = 0$. The solid line denotes the PDG bound on $BR(\mu \rightarrow e\gamma)$, while the dashed lines indicate the SINDRUM II limit on $\mu - e$ conversion and the projected MEG sensitivity to $BR(\mu \rightarrow e\gamma)$.

TeV are permitted with completely natural parameters. Super- B factory searches for rare τ decays will not significantly constrain scales $M_{KK} \geq 5$ TeV. The LHC search reach for the new states predicted by the anarchic RS scenario is expected to be around 5-6 TeV. It is therefore difficult to definitively test the RS geometric origin of flavor using data from B -factories and the LHC.

Searches for $\mu - e$ conversion and $\mu \rightarrow e\gamma$ are already starting to require slight tunings of the model parameters. The limit on $BR(\mu \rightarrow e\gamma)$ is projected to improve from 1.2×10^{-11} to 10^{-13} after MEG, while the constraint on $\mu - e$ conversion is projected to improve to 10^{-18} after PRIME. The bounds on M_{KK} that these constraints lead to are shown in Fig. 9. We have plotted the projected bounds as a function of the overall scale of the mixing angles; we have set $U_{12}^{L,R} = \kappa \sqrt{m_e/m_\mu}$, $U_{13}^{L,R} = \kappa \sqrt{m_e/m_\tau}$, etc., and have varied κ in the range $[0.01, 1]$. This tests how far from the natural parameters these experiments will probe. We observe that MEG will probe $M_{KK} \leq 5$ TeV down to mixing angles 1/10 times their natural sizes. PRIME will test $M_{KK} \leq 20$ TeV down to mixing angles 1/10 times their natural sizes, and will probe $M_{KK} \leq 10$ TeV down to mixing angles 1/100 times their canonical values. Together, these experiments will definitively test the anarchic RS explanation of the flavor sector.

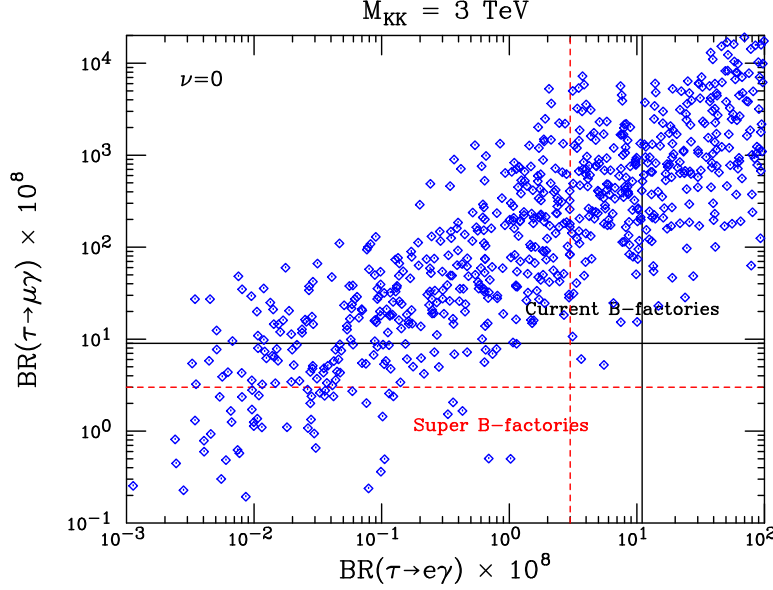


FIG. 7: Scan of the $\tau \rightarrow \mu\gamma$ and $\tau \rightarrow e\gamma$ predictions for $M_{KK} = 3$ TeV and $\nu = 0$. The solid and dashed lines are the current B -factory and projected super- B factory limits, respectively.

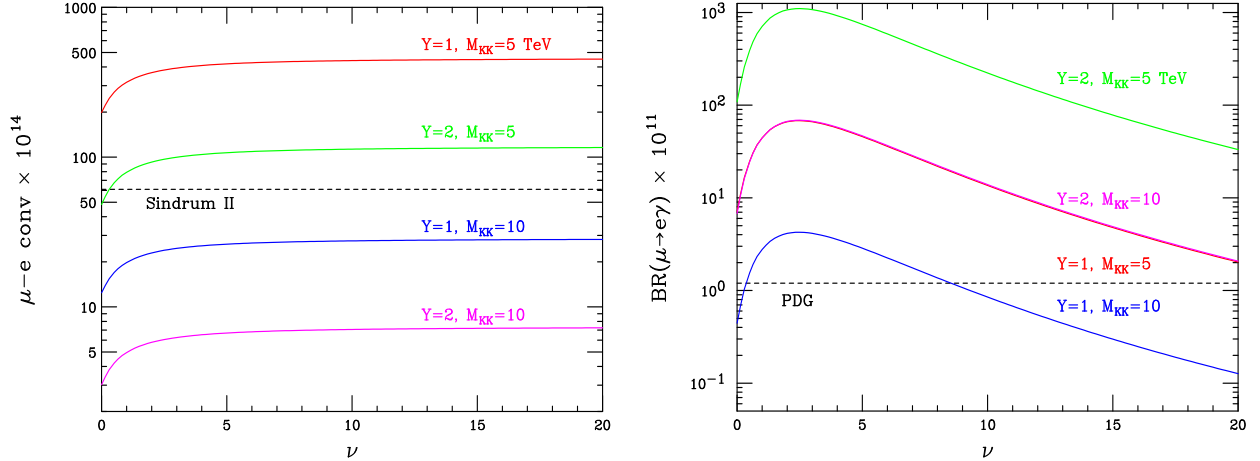


FIG. 8: ν dependence of the RS predictions for $\mu - e$ conversion and $\mu \rightarrow e\gamma$ for canonical mixing angles and for several choices of Y_x and M_{KK} . In the right panel, the $Y = 1$, $M_{KK} = 5$ TeV and the $Y = 2$, $M_{KK} = 10$ TeV lines overlap.

VI. SUMMARY AND CONCLUSIONS

In this paper, we have studied lepton flavor violation with the SM propagating in a warped extra dimension. The principal motivation for this model is a solution to the Planck-electroweak hierarchy problem. Interestingly, there is also a solution to the flavor hierarchy of the SM. The large differences in the quark and lepton masses and mixing angles can be explained by differing profiles of SM fermions in the extra dimension, even though the $5D$ Yukawa coupling are of the same size without any structure. These profiles can vary substantially with small changes in the $5D$ fermion masses; no large hierarchies are required to account for the flavor hierarchy in the SM. Since the Higgs field is localized near the TeV

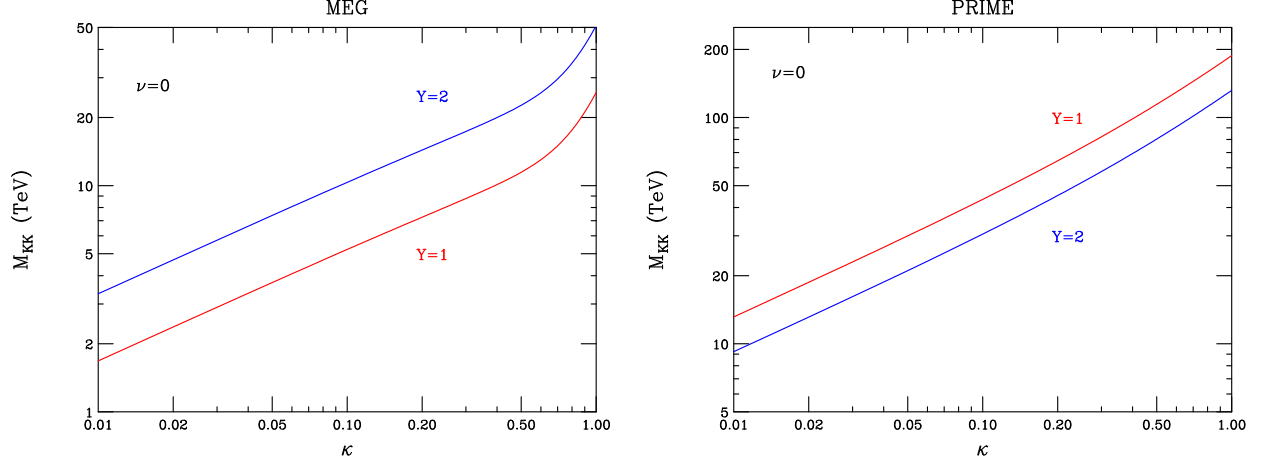


FIG. 9: Projected bounds on M_{KK} coming from MEG (left) and PRIME (right) for $\nu = 0$. We have set the mixing angles to κ times their canonical values, and have varied κ in the range $[0.01, 1]$ for $Y_x = 1, 2$.

brane, the small masses of the first and second generations are explained by their localization near the Planck brane.

The localization of fermion fields at different points in the extra dimension leads to flavor violation upon rotation to the fermion mass basis. The assumption of anarchic $5D$ Yukawa couplings implies that the mixing angles are related to the ratios of fermion masses. We can therefore estimate the leptonic mixing angles without a model of neutrino masses, unlike in the SM. The flavor violating couplings are proportional to the $4D$ Yukawa interactions. Therefore there is an analog of the GIM mechanism in the anarchic RS picture. However, the sensitivities of lepton flavor violating experiments are large, so we expect significant constraints. Bounds from electroweak precision measurements currently constrain the KK scale to be $M_{KK} \geq 3$ TeV, approximately.

To derive the implications of lepton flavor violating measurements for the anarchic RS scenario, we perform a Monte Carlo scan over the natural parameter space of this model: $O(1)$ Yukawa couplings and $O(1)$ variations of the mixing angles around their predicted size. We study both the case where the Higgs boson is localized in the TeV brane and when it is allowed to propagate in the full $5D$ spacetime. We study the processes $\mu \rightarrow 3e$, $\tau \rightarrow l_1 \bar{l}_2 l_3$, $\mu - e$ conversion, and dipole decays of the form $l \rightarrow l' \gamma$. In the brane Higgs case, cut-off effects render the dipole decays uncalculable in the $5D$ RS theory; this arises from the fact that the $5D$ Yukawa couplings in this case have mass dimension $[-1]$, and cut-off scale effects are as large as those from KK modes. The bulk Higgs case does not suffer from this drawback.

We find strong constraints throughout the entire natural RS parameter space. The minimal allowed KK scale is 3 TeV, and this is permitted only for a very few points in our scan. In the bulk Higgs case, this occurs partially because of a tension between the tree-level mediated $\mu - e$ conversion process and the loop-induced decay $\mu \rightarrow e \gamma$. These processes have opposite dependences on the $5D$ Yukawa couplings, making it difficult to decouple the effects of flavor violation. There are a couple of possible ways to avoid these constraints. First, the KK scale can be raised slightly to 5 TeV, which allows large regions of the natural RS parameter space to be realized. However, this increases the fine-tuning in the electroweak sector, and will make it difficult to find the KK states present in this model at the LHC.

Another possibility is to reduce the leptonic mixing angles slightly, implying some structure in the 5D Yukawa matrix and indicating that the observed flavor structure cannot be generated completely via geometry.

There are also several possible model-building possibilities to relax these constraints. Models with custodial isospin based on the gauge structure $SU(2)_L \times SU(2)_R \times U(1)_{B-L}$ contain an additional Z' and possibly additional fermions. The coupling of the Z' to the SM fermions is model-dependent [31], and can possibly be used to cancel some of the flavor-violating contributions we have studied. These models also contain an additional right-handed neutrino that contributes to loop-induced dipole decays. There is no zero-mode partner of this right-handed neutrino, and this contribution is therefore independent of the neutrino mixing parameters. Even an $O(1)$ suppression suffices to reduce the KK scale to the 3 TeV level, opening up more parameter space for study at the LHC.

The definitive test of whether the observed flavor structure can be explained by the anarchic RS scenario will come from future lepton flavor violating measurements. B -factories are currently probing mixing in the third generation using rare τ decays. These constraints will improve by an order of magnitude with data from a super- B factory, probing KK scales up to 5 TeV. These measurements probe different model parameters than $\mu-e$ conversion and rare μ decays, and are therefore complimentary to these other experiments. Improvements in the sensitivities of $\mu \rightarrow e\gamma$ and $\mu - e$ conversion of several orders of magnitude will be accomplished by the future experiments MEG and PRIME, respectively. They will definitively test the geometric origin of flavor structure; for example, PRIME will probe KK scales of $M_{KK} \geq 10$ TeV down to model parameters 1/100 of their natural size. These experiments will either confirm or completely invalidate this geometric origin of flavor.

In conclusion, the anarchic RS picture is an attractive solution to both the electroweak and flavor hierarchies in the SM. Measurements at the LHC, at future B -factories, and with the experiments MEG and PRIME will determine whether it is indeed realized in nature.

Acknowledgements

We thank R. Contino, H. Davoudiasl, D. E. Kaplan, R. Kitano and R. Sundrum for useful discussions. K. A. is supported in part by DOE grant DE-FG02-90ER40542. A. B. is partially supported by the U.S. National Science Foundation under grant PHY-0401513. F. P. is supported in part by the University of Wisconsin Research Committee with funds provided by the Wisconsin Alumni Research Foundation.

APPENDIX

In this Appendix we present the expressions that appear in the fermion mass and Yukawa coupling matrices. We focus on the case of a bulk Higgs field; the brane Higgs mass matrix can be obtained by taking the appropriate limits, as discussed below.

The fermion mass matrix for the bulk Higgs scenario is given by

$$\mathcal{M} = \begin{pmatrix} M_D & \frac{v}{\sqrt{2}}\Delta_R & 0 \\ \frac{v}{\sqrt{2}}\Delta_L & \Delta_1 & M_{KK} \\ 0 & M_{KK} & \Delta_2 \end{pmatrix}. \quad (54)$$

M_D is a 3×3 diagonal matrix containing the masses of the zero-mode leptons, and M_{KK} is the diagonal matrix with the KK masses before mixing. We assume that it is proportional to the identity matrix, as the deviation from this limit is small. The other entries can be expressed using the following two overlap integrals:

$$F^{ij} = \frac{\int_{-\pi}^{\pi} d\phi \chi_H(\phi) f_L^0(\phi; c_i) f_L^1(\phi; c_j)}{\int_{-\pi}^{\pi} d\phi \chi_H(\phi) f_L^0(\phi; c_i) f_L^0(\phi; c_j)}, \quad (55)$$

$$G_{L,R}^{ij} = \frac{\int_{-\pi}^{\pi} d\phi \chi_H(\phi) f_{L,R}^1(\phi; c_i) f_{L,R}^1(\phi; c_j)}{\int_{-\pi}^{\pi} d\phi \chi_H(\phi) f_L^0(\phi; c_i) f_L^0(\phi; c_j)}. \quad (56)$$

χ_H is the Higgs vev profile given in Eq. 16, while the $f^n(\phi; c_i)$ can be found in [7]. The remaining matrices in Eq. 54 are

$$\frac{v}{\sqrt{2}} \Delta_R^{ij} = U_{Lik} (U_L^\dagger M_D U_R)^{kj} \times F^{kj}, \quad (57)$$

$$\frac{v}{\sqrt{2}} \Delta_L^{ij} = (U_L^\dagger M_D U_R)^{ik} U_{Rkj}^\dagger \times F^{ki}, \quad (58)$$

$$\Delta_1^{ij} = (U_L^\dagger M_D U_R)^{ij} \times G_L^{ij}, \quad (59)$$

$$\Delta_2^{ij} = (U_L^\dagger M_D U_R)^{ij} \times G_R^{ij}, \quad (60)$$

where there is no sum over the indices i, j but there is over the index k .

To see how this reduces to the brane Higgs case, we replace the Higgs wavefunction with a delta function on the TeV brane. This sets $G_R = 0$ via the boundary conditions $f_R^1(\phi = \pi) = 0$, so that $\Delta_2 = 0$ as in Eq. 13. Also, $F^{ij} = F^j$, since the i flavor cancels out of the ratio in Eq. 55, and $G_L^{ij} = F^i F^j$, again matching our results for the brane Higgs.

We now discuss the diagonalization of this matrix and the fermion Yukawa coupling matrix. We first diagonalize the lower 2×2 block containing the KK masses, to remove the mixing between the KK fermions. We then diagonalize the full 3×3 matrix, to remove mixing between zero and KK modes. We include only the leading v/M_{KK} corrections.

We first consider the following simple 2×2 matrix, which simulates the lower block of Eq. 54:

$$T = \begin{pmatrix} x & 1 \\ 1 & y \end{pmatrix}. \quad (61)$$

We assume $x, y < 1$. This matrix is diagonalized by the following unitary transformation:

$$V = \frac{1}{\sqrt{2}} \begin{pmatrix} 1 + \frac{x-y}{4} & 1 - \frac{x-y}{4} \\ 1 - \frac{x-y}{4} & -(1 + \frac{x-y}{4}) \end{pmatrix}. \quad (62)$$

$VT V^\dagger$ is diagonal with eigenvalues $\pm(1 \pm \frac{1}{2}(x+y))$ to leading order in x and y . We now make this the lower 2×2 block of a diagonalization matrix V , identifying $X \equiv x - y = \frac{\Delta_1 - \Delta_2}{M_{KK}}$, and compute $\mathcal{M}_D = V \mathcal{M} V^\dagger$:

$$\mathcal{M}_D = \begin{pmatrix} M_D & \frac{v}{\sqrt{2}} \Delta_R \frac{1}{\sqrt{2}} (1 + \frac{X}{4}) & \frac{v}{\sqrt{2}} \Delta_R \frac{1}{\sqrt{2}} (1 - \frac{X}{4}) \\ \frac{1}{\sqrt{2}} (1 + \frac{X}{4}) \frac{v}{\sqrt{2}} \Delta_L & M_{KK} + \frac{\Delta_1 + \Delta_2}{2} & 0 \\ \frac{1}{\sqrt{2}} (1 - \frac{X}{4}) \frac{v}{\sqrt{2}} \Delta_L & 0 & -M_{KK} + \frac{\Delta_1 + \Delta_2}{2} \end{pmatrix}. \quad (63)$$

We now diagonalize the zero-KK mixing. We accomplish this with the following unitary transformation matrix:

$$Y = \begin{pmatrix} 1 & -\frac{v/\sqrt{2}}{M_{KK}}\Delta_R\frac{1}{\sqrt{2}}(1-\Gamma) & \frac{v/\sqrt{2}}{M_{KK}}\Delta_R\frac{1}{\sqrt{2}}(1+\Gamma) \\ \frac{1}{\sqrt{2}}(1-\Gamma)\frac{v/\sqrt{2}}{M_{KK}}\Delta_L & 1 & 0 \\ -\frac{1}{\sqrt{2}}(1+\Gamma)\frac{v/\sqrt{2}}{M_{KK}}\Delta_L & 0 & 1 \end{pmatrix}, \quad (64)$$

where $\Gamma = \frac{\Delta_1+3\Delta_2-4M_0}{M_{KK}}$. This removes the off-diagonal elements of the mass matrix. The eigenvalues are shifted at $\mathcal{O}(v/M_{KK})$; this will be important for the Yukawa matrix below. The full diagonalization matrix is YV . We must also include the phase rotation $P = \text{diag}(1, 1, -1)$ to make the eigenvalues positive. We can then determine the masses of the KK fermions to first order in v/M_{KK} :

$$M_{KK}^{(1)} = M_{KK} + \frac{\Delta_1 + \Delta_2}{2} \quad (65)$$

$$M_{KK}^{(2)} = M_{KK} - \frac{\Delta_1 + \Delta_2}{2} \quad (66)$$

These expressions for the KK masses are used when computing the amplitude for $\mu \rightarrow e\gamma$. The expression is valid for both the brane and bulk Higgs scenarios.

We now determine the Yukawa coupling matrix. The Yukawa matrix Λ in the flavor basis is obtained by dividing by $\frac{v}{\sqrt{2}}$ and setting $M_{KK} = 0$ in Eq. 54. Multiplying $YV\Lambda(YV)^\dagger P$, we obtain the Yukawa matrix in the mass basis

$$\Lambda_D = \begin{pmatrix} \lambda_{4D} & \frac{1}{\sqrt{2}}\Delta_R \left[1 + \left(\frac{X}{4} - \frac{\Delta_2 - M_0}{M_{KK}} \right) \right] & -\frac{1}{\sqrt{2}}\Delta_R \left[1 - \left(\frac{X}{4} - \frac{\Delta_2 - M_0}{M_{KK}} \right) \right] \\ \frac{1}{\sqrt{2}} \left[1 + \left(\frac{X}{4} - \frac{\Delta_2 - M_0}{M_{KK}} \right) \right] \Delta_L & \cdots & \cdots \\ \frac{1}{\sqrt{2}} \left[1 - \left(\frac{X}{4} - \frac{\Delta_2 - M_0}{M_{KK}} \right) \right] \Delta_L & \cdots & \cdots \end{pmatrix}. \quad (67)$$

We do not include the lower 2×2 block since we do not need it here. Note that $\Delta_2 \gg M_0$, so we can drop the dependence on the zero mode mass matrix in the off-diagonal terms. These correspond to subleading contributions suppressed by $1/f^2$.

-
- [1] L. Randall, R. Sundrum, *Phys. Rev. Lett.* **83**, 3370 (1999) [hep-ph/9905221].
 - [2] W. D. Goldberger and M. B. Wise, *Phys. Rev. Lett.* **83**, 4922 (1999) [arXiv:hep-ph/9907447].
 - [3] H. Davoudiasl, J. L. Hewett and T. G. Rizzo, *Phys. Lett. B* **473**, 43 (2000) [arXiv:hep-ph/9911262]. A. Pomarol, *Phys. Lett. B* **486**, 153 (2000) [arXiv:hep-ph/9911294].
 - [4] Y. Grossman, M. Neubert, *Phys. Lett.* **B474**, 361 (2000). [hep-ph/9912408]
 - [5] T. Gherghetta, A. Pomarol, *Nuc. Phys.* **B586**, 141 (2000). [hep-ph/0003129]
 - [6] S. J. Huber and Q. Shafi, *Phys. Lett. B* **498**, 256 (2001) [arXiv:hep-ph/0010195];
 - [7] H. Davoudiasl, J. L. Hewett and T. G. Rizzo, *Phys. Rev. D* **63**, 075004 (2001) [arXiv:hep-ph/0006041].
 - [8] S. J. Huber, *Nucl. Phys. B* **666**, 269 (2003) [arXiv:hep-ph/0303183].
 - [9] G. Burdman, *Phys. Lett. B* **590**, 86 (2004) [arXiv:hep-ph/0310144].
 - [10] S. Khalil and R. Mohapatra, *Nucl. Phys. B* **695**, 313 (2004) [arXiv:hep-ph/0402225].

- [11] K. Agashe, G. Perez and A. Soni, Phys. Rev. Lett. **93**, 201804 (2004) [arXiv:hep-ph/0406101]; Phys. Rev. D **71**, 016002 (2005) [arXiv:hep-ph/0408134].
- [12] G. Moreau and J. I. Silva-Marcos, JHEP **0603**, 090 (2006) [arXiv:hep-ph/0602155].
- [13] S. J. Huber and Q. Shafi, Phys. Rev. D **63**, 045010 (2001) [arXiv:hep-ph/0005286]; S. J. Huber, C. A. Lee and Q. Shafi, Phys. Lett. B **531**, 112 (2002) [arXiv:hep-ph/0111465]; C. Csaki, J. Erlich, J. Terning, Phys. Rev. **D66**, 064021 (2002) [hep-ph/0203034]; J. Hewett, F. Petriello, T. Rizzo, JHEP **0209**, 030 (2002) [hep-ph/0203091].
- [14] K. Agashe, A. Delgado, M. May, R. Sundrum, JHEP **0308** 050 (2003). [hep-ph/0308036]
- [15] H. Davoudiasl, J. L. Hewett and T. G. Rizzo, Phys. Rev. D **68**, 045002 (2003) [arXiv:hep-ph/0212279]; M. Carena, E. Ponton, T. M. P. Tait and C. E. M. Wagner, Phys. Rev. D **67**, 096006 (2003) [arXiv:hep-ph/0212307]; M. Carena, A. Delgado, E. Ponton, T. M. P. Tait and C. E. M. Wagner, Phys. Rev. D **71**, 015010 (2005) [arXiv:hep-ph/0410344].
- [16] K. Agashe, R. Contino and A. Pomarol, Nucl. Phys. B **719**, 165 (2005) [arXiv:hep-ph/0412089].
- [17] H. Davoudiasl, B. Lillie and T. G. Rizzo, arXiv:hep-ph/0508279.
- [18] G. Signorelli, J. Phys. G **29**, 2027 (2003).
- [19] A. Sato, talk given at 7th International Workshop on Neutrino Factories and Superbeams (NuFact 05), Frascati, Italy, 21-26 Jun 2005.
- [20] R. Kitano, Phys. Lett. B **481**, 39 (2000) [arXiv:hep-ph/0002279].
- [21] W. F. Chang and J. N. Ng, Phys. Rev. D **71**, 053003 (2005) [arXiv:hep-ph/0501161].
- [22] Y. Kuno and Y. Okada, Rev. Mod. Phys. **73**, 151 (2001) [arXiv:hep-ph/9909265].
- [23] P. Wintz, Prepared for 29th International Conference on High-Energy Physics (ICHEP 98), Vancouver, Canada, 23-29 Jul 1998
- [24] S. Eidelman *et al.* [Particle Data Group], Phys. Lett. B **592**, 1 (2004).
- [25] Y. Yusa *et al.* [Belle Collaboration], Phys. Lett. B **589**, 103 (2004) [arXiv:hep-ex/0403039]; M. Hodgkinson [BaBar Collaboration], Nucl. Phys. Proc. Suppl. **144**, 167 (2005).
- [26] H. Davoudiasl, J. L. Hewett and T. G. Rizzo, Phys. Lett. B **493**, 135 (2000) [arXiv:hep-ph/0006097].
- [27] K. Abe *et al.* [Belle Collaboration], Phys. Rev. Lett. **92**, 171802 (2004) [arXiv:hep-ex/0310029]; J. M. Roney [BaBar Collaboration], Nucl. Phys. Proc. Suppl. **144**, 155 (2005) [arXiv:hep-ex/0412002].
- [28] K. Hayasaka *et al.*, Phys. Lett. B **613**, 20 (2005) [arXiv:hep-ex/0501068]; B. Aubert *et al.* [BABAR Collaboration], Phys. Rev. Lett. **96**, 041801 (2006) [arXiv:hep-ex/0508012].
- [29] J. Hewett (ed.), *et al.*, arXiv:hep-ph/0503261.
- [30] N. G. Unel, arXiv:hep-ex/0505030.
- [31] K. Agashe, R. Contino, L. Da Rold and A. Pomarol, arXiv:hep-ph/0605341.